REVIEW ARTICLE OPEN

Check for updates

Advances in flexible organic field-effect transistors and their applications for flexible electronics

Kai Liu[1,2], Bang Ouyang[3], Xiaojun Guo[3 ✉], Yunlong Guo[1,2 ✉] and Yunqi Liu[1,2]

Flexible electronics have suggested tremendous potential to shape human lives for more convenience and pleasure. Strenuous efforts have been devoted to developing flexible organic field-effect transistor (FOFET) technologies for rollable displays, bendable smart cards, flexible sensors and artificial skins. However, these applications are still in a nascent stage for lack of standard high-performance material stacks as well as mature manufacturing technologies. In this review, the material choice and device design for FOFET devices and circuits, as well as the demonstrated applications are summarized in detail. Moreover, the technical challenges and potential applications of FOFETs in the future are discussed.

INTRODUCTION

Flexible electronics, as an emerging and vigorous research field, have garnered considerable attention in the past decades due to their promising application in rollable display screens, intelligent identification cards, and on-body wearable and implantable electronics[1–3]. The term flexible electronic refers to a special class of thin-film electronic devices that can retain comparatively steady electrical performance when subjected to mechanical bending, folding, twisting, compression and stretching[4]. Thus far, a striking progress has been achieved in various flexible electronic devices, such as organic light-emitting diodes (OLEDs), organic field-effect transistors (OFETs), organic photovoltaics (OPVs), organic sensors, and memories. Thereinto, OFETs that are also organic thin-film transistors (OTFTs), are characterized with inherent flexibility, light weight, low-power consumption, ease of integration, high sensitivity, large-area solution manufacturing, and simultaneously function as switches, amplifiers, transducers, drivers, and data-storage components for rollable displays, bendable smart cards, conformable sensors and artificial skins[5–16] (Fig. 1). For example, compared with resistor-type sensors, OFET-based sensors generally exhibit higher sensitivity due to their signal amplification and tuning under applied gate voltage (V_{GS})[17]. Moreover, owing to the ease of miniaturization and integration, OFETs have great potential as a critical unit for building flexible digital circuit blocks and microprocessors[4].

For flexible OFETs (FOFETs), all components must have certain mechanical compliance and strength. Unlike conventional Si-based OFETs mainly considering the electrical properties, FOFETs are evaluated by comprehensively considering the trade-off between electronic properties and mechanical flexibility. Through the continuous efforts and exploration of researchers, three strategies have been proposed to enhance the strain-tolerance capacity of FOFET circuits. The first one is to develop intrinsically flexible or stretchable organic materials with low elastic modulus. FOFETs based on the intrinsically flexible materials are advantageous to achieve scalable fabrication, higher device integration density, and superior strain tolerance. Thereinto, incorporating either soft segments or dynamic interactions in polymer molecular chains is the most straightforward method to enhance the flexibility of polymer materials[18]. In addition, blending with elastomers and conducting fillers are also a simple and effective strategy to fabricate intrinsically flexible or stretchable organic materials[19]. The second one is to design a particular geometric configuration of organic materials based on strain-engineering strategy. The structural engineering is considered as a common approach to afford materials with higher strain tolerance. For example, the materials are designed with various flexible interconnects (such as serpentine, spring-like, kirigami, horseshoe, textile, origami), or the devices are constructed on pre-strained elastomeric substrate[20,21]. The third one is to develop efficient processing techniques. Compared with traditional spin-coating and vacuum-thermal evaporation, high-throughput processing approaches, such as doctor-blade coating, slot die coating, screening, and gravure printing, might be better to enable large-area manufacturing of FOFET integrated circuits[22–25]. Meanwhile, the thermal lamination-transfer technique is typically employed to prepare intrinsically stretchable organic transistors and arrays, which is conducive to avoid the solvent damage and metal penetration[26–28].

Over the past two decades, great success has been witnessed in high-performance FOFETs and their applications in flexible electronics. The aim of this review is to provide a detailed and up-to-date introduction about FOFETs with structural design strategies and material selection considerations, as well as their various promising applications. In order to make readers better understand the FOFETs, we shall first focus on how the OFETs work under applied voltage, how to simultaneously improve the electrical performances and mechanical compliance of FOFETs, how to design device configurations of FOFETs, and how to determine the appropriate materials and device assembly techniques for FOFETs. Subsequently, the progress of FOFETs in flexible organic circuits and the requirements for large-scale circuitry are introduced in detail. Moreover, some existing and potential applications, including rollable display, conformable sensor array, bendable smart cards, and artificial skin, are summarized. Lastly, some conclusions and prospects are discussed

[1]Beijing National Laboratory for Molecular Sciences, Key Laboratory of Organic Solids, Institute of Chemistry, Chinese Academy of Sciences, 100190 Beijing, People's Republic of China. [2]School of Chemical Sciences, University of Chinese Academy of Sciences, 100049 Beijing, People's Republic of China. [3]Department of Electronic Engineering, School of Electronic Information and Electrical Engineering, Shanghai Jiao Tong University, 200240 Shanghai, People's Republic of China. ✉email: x.guo@sjtu.edu.cn; guoyunlong@iccas.ac.cn
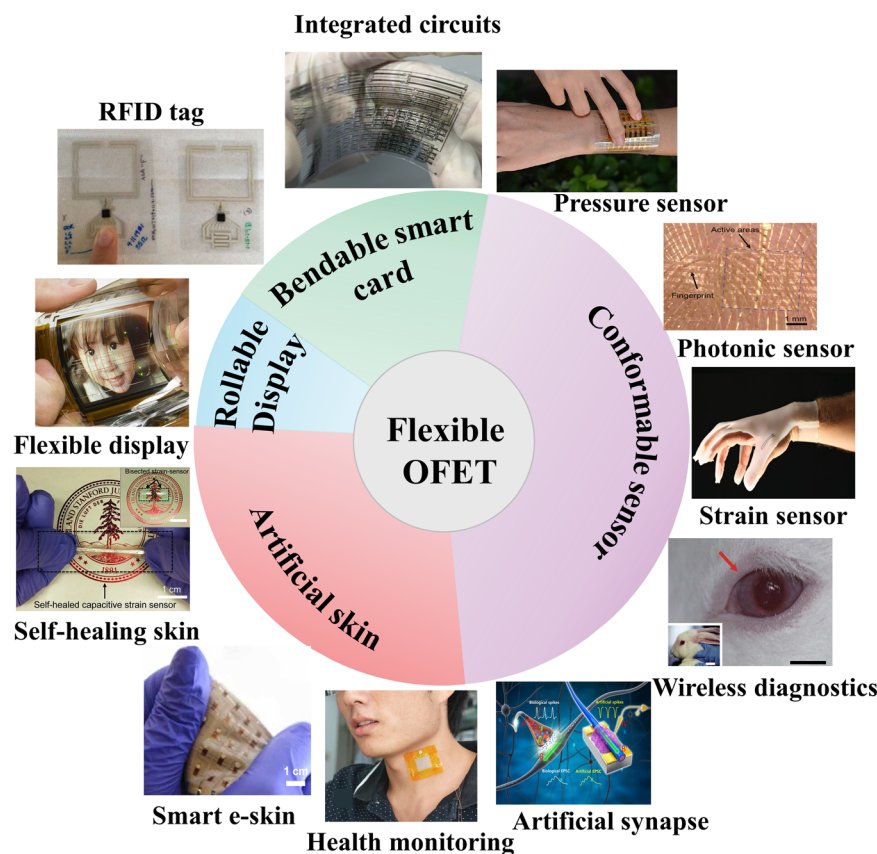
Fig. 1   Representative application examples of flexible OFETs. 'Flexible display:' Reproduced with permission[6]. Copyright 2012, Wiley-VCH. 'RFID tag:' Reproduced with permission[7]. Copyright 2020, Springer Nature. 'Integrated circuits:' Reproduced with permission[8]. Copyright 2019, Springer Nature. 'Pressure sensor:' Reproduced with permission[9]. Copyright 2015, Springer Nature. 'Photonic sensor:' Reproduced with permission[10]. Copyright 2021, Wiley-VCH. 'Strain sensor:' Reproduced with permission[11]. Copyright 2014, Wiley-VCH. 'Wireless diagnostics:' Reproduced with permission[12]. Copyright 2017, Springer Nature. 'Artificial synapse:' Reproduced with permission[13]. Copyright 2016, American Association for the Advancement of Science. 'Health monitoring:' Reproduced with permission[14]. Copyright 2014, Wiley-VCH. 'Smart e-skin:' Reproduced with permission[15]. Copyright 2020, American Association for the Advancement of Science. 'Self-healing skin:' Reproduced with permission[16]. Copyright 2018, Wiley-VCH.

at the end of this review to provide insights into the future research of flexible electronics.

STRATEGIES FOR FOFETS

In order to deepen readers' understanding of FOFETs, this section first focuses on the device architectures and working mechanisms of OFETs. Conventional OFETs are three-terminal electronic devices composed of organic semiconductor layer, gate dielectric layer, source/drain (S/D) electrodes, and gate electrode. Certainly, all the components should be supported by a substrate. According to the position of gate electrodes and S/D electrodes relative to semiconductor layer, OFETs are distinguished as four types: bottom-gate bottom-contact (BGBC) configuration, bottom-gate top-contact (BGTC) configuration, top-gate bottom-contact (TGBC) configuration, and top-gate top-contact (TGTC) configuration. In addition, some special cases, such as dual-gate[29] and side-gate[30] configurations, have been also reported. For the TC configuration, organic semiconductors are directly grown or deposited onto the dielectric layer, followed by the deposition of source and drain electrodes, which ensures good crystal structures and the uniform semiconductor/dielectric contact interface. However, for the BC configuration, organic semiconductors are grown or deposited onto the S/D electrodes and gate dielectrics, thereby resulting in the performance and structure discrepancies. Comparing with BC configuration, the TC configuration exhibits a larger contact area and lower contact resistance

between semiconductors and electrodes[31]. But the TC configuration is difficult to realize mass production due to the restricted mask technologies, which is not fit for practical application.

The charge density in the active channel is regulated by the electric perpendicular field. To further explore the field-effect characteristics of OFETs, the threshold voltage (V_{th}), charge mobility (μ), I_{on}/I_{off}, and subthreshold slope (SS), should be extracted from the transfer ($I_{SD} - V_G$) and output ($I_{SD} - V_{SD}$) curves. But for FOFETs, there still exist additional parameters, including device thickness, curvature radius, stretching strain, and electrical stability against mechanical deformations, meriting considerable attention. Next, we will summarize the standard high-performance material stacks (including organic semiconductors, electrodes, gate dielectrics, and substrates) for FOFETs.

Organic semiconductors for FOFETs

Organic semiconductors (OSCs) are acknowledged as the core components of OFETs. The carrier mobility of OFETs was significantly dependent on both the chemical structures of conjugated frameworks and the intermolecular π-orbital overlapping[32,33]. OSCs are classified as organic molecules, oligomers, and conjugated polymers. Thereinto, oligomers are seldomly investigated due to their inferior electrical characteristics, uneasy purification, and processing. By contrast, organic molecules and conjugated polymers have been extensively applied in flexible electronic devices due to their good flexibility, high molecular

density, low cost, low-temperature processability, and outstanding compatibility with flexible substrate[34]. Because of less grain boundaries as well as less defects and traps, organic molecules exhibit comparable mobility to polycrystalline silicon FETs (>10 cm^2 V^{-1} s^{-1}), such as 2,9-didecyl-dinaphtho[2,3-b:20,30-f]thieno [3,2-b]thiophene (C10-DNTT, 10.7 cm^2 V^{-1} s^{-1})[35], rubrene (24.5 cm^2 V^{-1} s^{-1})[36], and C8-BTBT (31.3 cm^2 V^{-1} s^{-1})[37]. Moreover, organic single crystals are seen as the desirable materials to systematically explore the relationship between electronic characteristics and mechanical performances. Reyes-Martinez[38] used rubrene as the benchmark semiconductor to explore how the mechanical deformations impact the carrier mobility due to the ignorable grain boundaries and defects. They discovered that the mechanical tension increased the intermolecular distance and decreased the carrier mobility of the rubrene single-crystal FETs, whereas mechanical compression was the opposite. Moreover, the net strain at the dielectric/semiconductor interface would also influence the carrier mobility. While not as abundant as polymer semiconductor examples, the research of organic molecules for fabricating FOEFTs still attracted considerable attention.

Comparing with organic small molecules, polymer semiconductors show higher molecular weight, controllable molecular structure, superior mechanical flexibility, and good film-assembling capability[39]. Moreover, both highly ordered lamellar structure and high crystallinity are beneficial for the increase of carrier mobility of polymer semiconductors, but they are detrimental to the mechanical stretchability that thirsts for an amorphous morphology[40]. As a representative example, poly(3-hexylthiophene) (P3HT), with plenty of side-chain regions, contains a lamellar packing pattern of conjugated backbones and its ring planes adopt edge-on stacking along the substrate. Whereas poly-(2,5-bis(3-alkylthiophene-2-yl)thieno [3,2-b]thio-phene) (pBTTT) more easily forms highly ordered films due to the existence of many crystalline domains with larger crystalline sizes and fewer defects. The molecular packing geometries for the crystalline region of polymer P3HT and pBTTT are shown in Fig. 2a. Therefore, pBTTT exhibits higher carrier mobility, but rather lower crack onset strain (<2.5%) comparing with P3HT (>150%). These results illustrate that long-range order is preferable to increase mobility, but inevitably stiffens and embrittles the polythiophene semiconductor films[41]. Wu et al.[42] proposed a facile and effective strategy to investigate the flexibility and stretchability of polymer semiconductors through soft contact lamination. They found that comparing with large-scale fused rings, the free thiophene rings and long branched alkyl side chains could generate larger free volume, which was conducive to improve the stretchability and crack onset strain of polymer semiconductors.
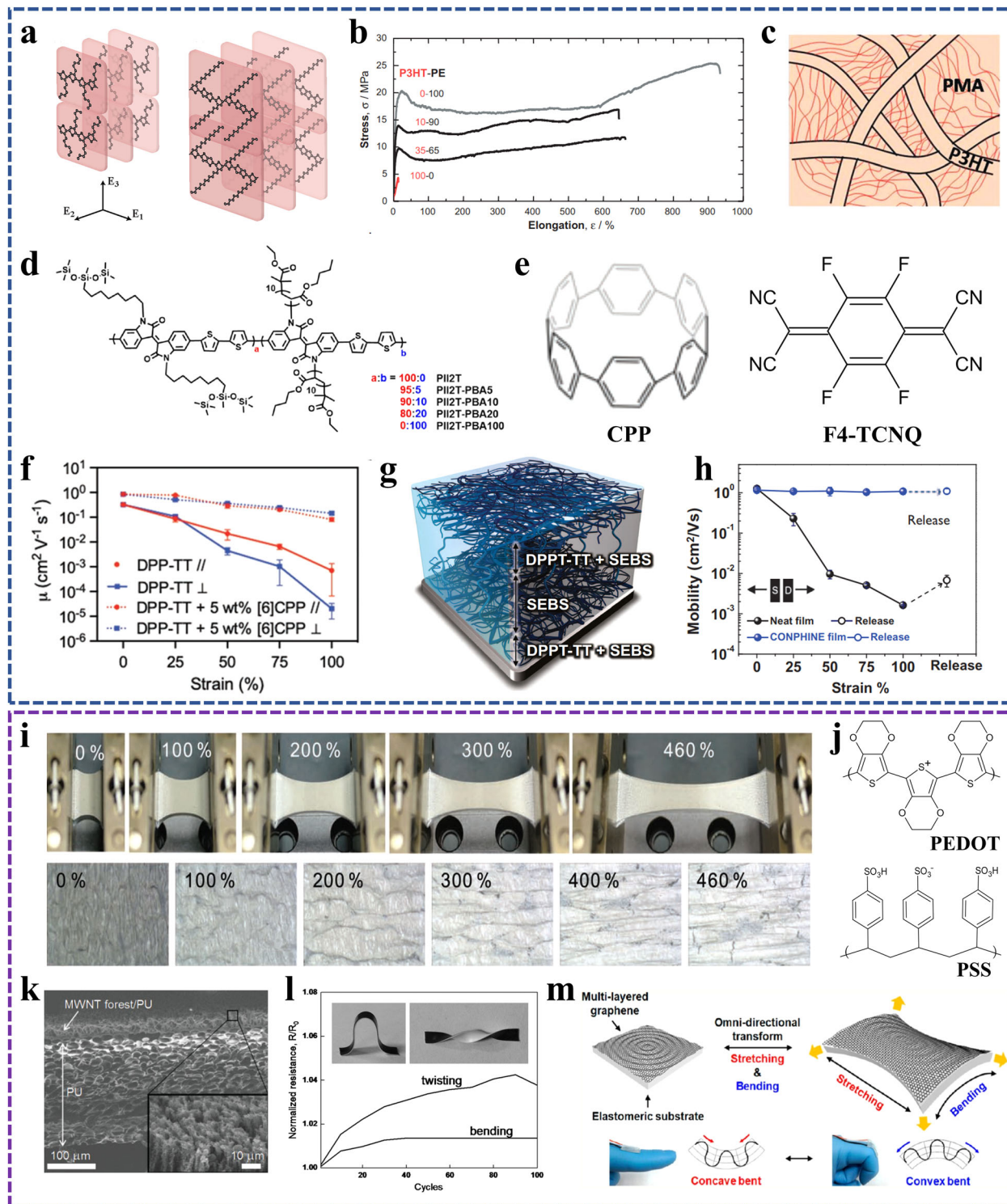
Taking together, good electrical performance and good mechanical compliance in polymer semiconductors are difficult to balance. Current approaches to increase the flexibility and stretchability of polymer semiconductors were primarily on the basis of six categories: (1) designing multiblock copolymers by incorporating flexible or elastic insulating segments into polymer backbone, so as to reduce the π–π stacking and crystallinity of polymer semiconductors. P3HT-PE diblock copolymer (crack onset strain > 600%)[43] (Fig. 2b) and P3HT-PMA-P3HT triblock copolymer (rack onset strain > 140%) (Fig. 2c)[44] are two representative examples. (2) Incorporating alkyl side chains to weaken inter-molecular interactions and localize aggregates in conjugated polymers[45,46]. For example, the introduction of poly (butyl acrylate) (PBA) side chains into isoindigo-bithiophene (II2T)-based conjugated polymers could provide better processability, lower elastic modulus, and superior mechanical ductility for polymer semiconductors[47]. The chemical structure of PII2T-PBA with different molar ratios of PII2T and PBA is shown in Fig. 2d. (3) Regulating molecular weight (M_n) and regioregularity (RR) of polymer semiconductors. Several reports have confirmed that the increasing M_n and decreasing RR could improve the strain

tolerance of polymer semiconductors[48,49]. (4) Introducing conjugated carbon cyclic nanorings as additives into polymer semiconductors, which can suppress the formation of large crystallites and facilitate the formation of small aggregates, thereby increasing the flexibility and carrier mobility of polymer semiconductors. For instance, polymer DPP-TT with the inclusion of cycloparaphenylene (CPP)[19] (Fig. 2f) and 2,3,5,6-tetrafluoro-7,7,8,8-tetracyanoquinodimethane (F4-TCNQ)[50] could withstand high stretching strain up to 100% with minimal degradation of carrier mobility. The chemical structures of molecular additive CPP and F4-TCNQ are shown in Fig. 2e. (5) Blending with elastomers to improve chain dynamics and suppress large crystallites of polymer semiconductors. Blends consisting of conjugated polymers and elastomers are considered as the desirable hybrid polymer semiconductors with simultaneously increased mechanical stretchability and carrier mobility, and have been frequently employed to prepare stretchable transistors[51,52]. For instance, Xu and coworkers[26] proposed a conjugated-polymer/elastomer phase separation-induced elasticity (CONPHINE) methodology based on the nanoconfinement effect (Fig. 2g). The resulting hybrid polymer semiconductor could sustain high tensile strain up to 100% without sacrificing the carrier mobility (Fig. 2h). However, in the blending processes, the surface energies, molecular weight, blending ratio, solvents, and processing methods should be addressed. (6) Geometrically structuring the conventional brittle polymer semiconductors through strain-engineering designs, such as wave, wrinkle, island-bridge, textile, origami, kirigami, interlock, horseshoe, and serpentine shapes[20,53]. The strain-engineering design could improve the mechanical durability of polymer semiconductors to a certain extent, but also shows some drawbacks, such as limitation in the stretching strain (generally < 20%) due to unchanged polymer molecular structure, tedious processing procedures, low device density, and hard to large-area manufacturing.

Electrodes for FOFETs

Flexible electrodes, as another essential research consideration in FOFET design, have also raised tremendous research interest. To enable high-performance FOFETs, several pivotal requirements including high flexibility and transparency, superior conductivity, suitable work function, low contact resistance with semiconductors, and desirable biocompatibility, should be underlined[54]. Indium tin oxide (ITO) films are electrically conductive and optically transparent, and have been extensively used in optoelectronics for a few decades. Nevertheless, ITO films are stiff and brittle, and readily rupture when suffering from small stretching strains. In addition, various metal (e.g., Au, Ag, and Al) films are also the commonly used electrode materials due to high conductivity and transparency. Previous studies on flexible electronics usually employed metal films as flexible electrodes, and indicated that decreasing the thickness of metal films could endure small-scale mechanical bending and stretching. However, the reduction of metal film thickness typically induced the generation of isolated metal islands due to the Ostwald ripening effect, thereby resulting in the loss of electrical conductivity[55,56]. In order to catch up with the rapid development of wearable electronics, various flexible electrodes, including metal nanoparticles, metal nanowires, conductive polymers, carbon-based nanomaterials, and ionic conductors, have been reported[54,55,57].

Metal nanoparticles (NPs) and metal nanowires (NWs) not only maintain the excellent conductivity of metal films, but also show the improved mechanical flexibility and stretchability[58–60]. Generally, metal NPs, as 0D conductive nanomaterials, should be incorporated into elastomer matrix to obtain stretchable electrodes. For example, Kim et al.[61] prepared highly conductive stretchable electrodes by introducing Ag NPs in the PDMS matrix. The resulting electrodes displayed a low surface resistance of

0.910 Ω sq^{-1} and a high stretchability up to 100% strain with minimal degradation in electrical conductivity. Among metal NWs, silver nanowires (AgNWs) are the most commonly used flexible electrode materials due to high aspect ratio, excellent light transmittance (≈89%), and outstanding strain resistance. Moreover, the AgNW inks and films with a wide range of aspect ratios have been commercialized, making them a promising candidate for flexible and stretchable electrodes. However, the metal NW films display a high sheet resistance due to large wire–wire junction resistance[62]. The sheet resistance severely increases under stretching and bending deformations because of the fracture of wire–wire junctions. Lee and coworkers[63] developed a low-temperature successive multistep growth (SMG) approach to prepare ultra-long AgNWs. The high aspect ratio of AgNWs was beneficial for the balance of electrical conductivity and mechanical compliance. Thus, the resulting ultra-long AgNW percolation network (VAgNPN) electrodes retained a record-high stretching strain above 460% with insignificant reduction of sheet resistance

Fig. 2   Material design strategy for flexible OFETs. a Schematic diagram illustrating the molecular packing geometry for the crystalline region of polymer P3HT (left) and pBTTT (right). Reproduced with permission[41]. Copyright 2010, American Chemical Society. **b** Stress-elongation curves of the diblock copolymers with different weight ratios of P3HT and PE. Reproduced with permission[43]. Copyright 2007, Wiley-VCH. **c** Schematic diagram representing the configuration of P3HT-b-PMA-b-P3HT triblock copolymer. Reproduced with permission[44]. Copyright 2015, Royal Society of Chemistry. **d** Chemical structure of PII2T-PBA polymer with different molar ratios of PII2T and PBA. Reproduced with permission[47]. Copyright 2017, American Chemical Society. **e** Chemical structure of molecular additive CPP and F4-TCNQ. 'CPP:' Reproduced with permission[19]. Copyright 2019, Wiley-VCH. **f** Carrier mobilities of intrinsically stretchable OFETs prepared with polymer DPP-TT/CPPs hybrid film as the semiconductor layer under stretching strain up to 100% parallel and perpendicular to the charge transport direction. Reproduced with permission[19]. Copyright 2019, Wiley-VCH. **g** 3D schematic diagram illustrating the dispersion of DPPT-TT polymer in the SEBS matrix for the CONPHINE film. **h** Comparison in the carrier mobilities of the neat DPPT-TT film and CONPHINE film under 100% tensile strain along the charge transport direction. Reproduced with permission[26]. Copyright 2017, American Association for the Advancement of Science. **i** Macroscopic (top) and microscopic (bottom) surface morphologies of the ultra-long VAgNPN electrodes under stretching strain from 0 to 460%. Reproduced with permission[63]. Copyright 2012, Wiley-VCH. **j** Chemical structures of polymer PSS and PEDOT. **k** Scanning electron microscope (SEM) image of the MWNT/PU composite electrode. A highly porous foam morphology is demonstrated in the high-magnification SEM image. **l** Sheet resistance of the MWNT/PU composite electrode under multiple twisting and bending cycles. Reproduced with permission[70]. Copyright 2010, Wiley-VCH. **m** Multilayered graphene electrodes on the PDMS substrate against omnidirectional stretching and convex-concave bending. Reproduced with permission[73]. Copyright 2016, American Chemical Society.

(Fig. 2i). Meanwhile, the preparation approach was also promising for enabling low-cost, mass-production, and high-flexibility stretchable electrodes.

Conducting polymers (CPs), including polyaniline (PANI)[64] and poly(3,4-ethylenedioxythiophene) (PEDOT)[65], are desirable flexible electrode materials. Moreover, better conducting polymers can be enabled by blending different ones. Thereinto, Poly(3,4-ethylene-dioxythiophene):polystyrene sulfonate (PEDOT:PSS) is the most extensively used CPs in flexible electronics owing to their good mechanical strength, electrical stability and optical transmittance, as well as excellent film uniformity and attractive biocompatibility. The chemical structures of PEDOT and PSS are shown in Fig. 2j. The PEDOT:PSS film can also be easily patterned by inject printing, photolithography, selective wetting-based patterning, screen printing, etc[66]. However, pristine PEDOT:PSS film is susceptible to humidity, and is vulnerable to stretching strain (<5%). To address this conundrum, some effective strategies, such as the incorporation of elastomeric materials, surfactants, structural engineering, and the formation into micro/nanostructures, have been proposed[67].

Carbon-based nanomaterials mainly contain one-dimensional carbon nanotubes (CNTs) and two-dimensional graphene. Thereinto, CNTs have some distinctive characteristics such as excellent electrical conductivity ($\approx 10^4$ S cm^{-1}), superior mechanical robustness, outstanding thermal stability and low sheet resistance (<100 Ω)[68]. A single nanotube typically shows fairly ballistic transport with a current level approaching 25 μA per tube and a high tensile modulus up to 100 GPa. Since 2005, CNTs have been widely used as electrode materials for flexible electronics. Highly flexible and conductive CNT electrodes are usually prepared onto the flexible and stretchable substrates through drop-casting, spray-casting, or spin-coating methods. For example, Lipomi et al.[69] prepared a spring-like SWCNT electrode with high stretchability, transparency and conductivity by firstly imposing stretching strain along each axis and subsequently releasing this strain. The resulting SWCNT electrodes exhibited high stretching strain exceeding 150% and high conductivity up to 2200 cm^{-1}. But inevitably, high surface roughness from plenty of nanotube stacking on flexible or elastomeric substrate results in the deterioration of contact interface and the increase of contact resistance, thereby degrading the electrical performances of FOFETs. To solve this problem, Shin et al.[70] reported an elastomeric conductive composite by infiltrating multiwalled CNT (MWCT) forest using a polyurethane (PU) solution in N,N-dimethylformamide (DMF). The PU could totally penetrate the MWCT forest side, and the PU layer was interconnected with the forest to generate a highly porous foam (Fig. 2k). The resulting composite electrode film could sustain a stretching strain of 20% and multiple twisting deformations 100 times without sacrificing the sheet resistance (Fig. 2l).

Graphene, as a one-atom-thick 2D layer of sp2-bonded carbon allotrope, demonstrates excellent electrical-mechanical properties, low sheet resistance (100–1000 Ω sq^{-1}), and ideal optical transparency (>90%)[71]. Nevertheless, high in-plane stiffness (>340 N m^{-1}) and Yong's modulus (>0.5 TPa), as well as the strong internal C–C networks largely restrict its application in flexible and stretchable electronics[72]. Hong et al.[73] proposed a facile and cost-effective Fresnel lens-patterned method to achieve a concentric circular wavy configuration for the multilayered graphene sheets. The resulting graphene electrodes were afforded with high optical transmittance (>87% at 550 nm), low sheet resistance, and good strain tolerance to omnidirectional stretching (up to 30% tensile strain) (Fig. 2m). However, both the CNT and graphene have their merits and demerits. Therefore, researcher have also devoted great efforts to prepare hybrid electrodes with combined advantages, such as AgNWs/PEDOT:PSS[74], AgNWs/CNT[75], and AgNWs/rGO[76].

Ionic conductors and metal liquid are two new types of flexible electrodes. Ionic conductors, a hydrogel with plenty of slats, show ultrahigh transparency of approaching 100%, high stretching strain of 100–1000%, high operation frequency of exceeding 10 kHz, and superior biocompatibility[77]. However, the rather higher sheet resistance than other electrode materials, and the inevitable dehydration make it difficult to work as electrode materials in flexible electronics. Metal liquid combines the conductivity of metal with the fluidity of liquids[78]. But the unsatisfactory characteristics with inferior chemical stability, high sheet resistance, and uncontrollable liquidity, should be further overcome.

Dielectrics for FOFETs

The carrier transmission resides at two to three semiconducting molecular layers of the semiconductor-dielectric interfaces. The roughness and surface energy of dielectric layer obviously impact the growth process and morphology of organic semiconductors. Therefore, how to select suitable dielectric materials is also a critical consideration for high-performance FOFETs. Conventional inorganic oxides such as SiO$_2$ cannot be used as flexible dielectric materials due to their brittle and stiff nature. By contrast, polymer dielectrics are afforded with some inherent advantages, including low-temperature solution processing, low film density, high leakage current density, good compatibility with flexible substrate, controllable molecular structures, and molecular weight[79]. Currently, common flexible polymer dielectrics contain poly (methyl methacrylate) (PMMA)[3], polystyrene (PS)[6], and poly (α-methylstyrene) (PαMS)[4]. Common stretchable polymer dielectrics contain poly(dimethylsiloxane) (PDMS)[19] and polystyrene-block-poly

(ethylene-ran-butylene)-block-polystyrene (SEBS)[26]. However, these polymer dielectric materials show lower dielectric constant ($\kappa < 3.0$) comparing with inorganic rigid dielectrics, which resulted in the increased operation voltage of FOFETs. It cannot satisfy the low energy-consumption requirements of wearable electronic devices. The inclusion of conducting fillers and metal ions can effectively increase the κ of polymer dielectrics[80]. Additionally, the inferior solvent resistance of polymer dielectrics is also a considerable challenge. A commonly used strategy to overcome this issue is on basis of the crosslinking of polymer dielectrics (such as azide-crosslinking SEBS)[81].

Substrates for FOFETs
Flexible substrates play a supporting role for all the components of FOFETs. Currently reported flexible substrates consist of thin glass, metal foil, polymers (plastics and elastomers), and some special cases such as paper, fiber. Similar to polymer dielectrics, polymer substrates have some natural merits. To avoid solvent damage, polymer substrates should be imparted with superior thermal resistance and solvent resistance to harsh solvents. Unlike plastics, elastomeric polymers are easily subjected to dimensional deformation under high temperature and solvent damage due to their low glass transition temperature and high molecular dynamics. Therefore, if elastomeric substrate is involved, novel device assembly techniques (such as lamination-transfer procedures) should be employed. Meanwhile, future requirements for ultra-thin and ultra-flexible FOFETs are also dependent on the thickness of polymer substrates. In terms of the aforementioned flexible semiconductors, electrodes, dielectrics, and substrates, high-performance FOFET circuits and their applications in flexible electronics have been reported, which will be discussed in the following section.

FLEXIBLE CIRCUITRY
In recent years, OFETs have made extraordinary progress in integrated circuits. Since the flexible organic circuits were reported for the first time in 1998[82], the flexible integrated systems have attracted much attention and were rapidly developed from unipolar organic circuits to complementary organic circuits. The suitable materials and available device assembly technologies for large-scale and practically applicable circuitry are highly desirable[83].

In the design of silicon-based transistor integrated circuit, the complementary circuit composed of n-type and p-type transistors has the advantages of low static power consumption, rail-to-rail voltage output, high noise margin, and high gain[84]. However, for OFETs, it is difficult to obtain n-type and p-type OSC materials with matching performance and the integration process is also complex. Therefore, the full p-type circuits are in wide use because of its simple processing technology. The simplest form of a full p-type circuit is composed of two OFETs, where the load OFETs can be either gate and drain short-circuitry (enhanced load) or gate and source short-circuitry (depleted load), depending on the V_{th} of the OFETs. However, this kind of circuit design has the problems of low noise margin and hardly achieving rail-to-rail voltage output[85]. In order to improve the performance, the pseudo-CMOS structure is expected to achieve high noise tolerance and high gain.

According to the function of circuits, they are divided into digital, analog, and mixed circuits. The digital and analog circuits are the two most commonly used types. Generally, digital circuit has a large integrated scale, and it is easier to adopt standard cell to improve the design efficiency. The commonly used digital unit circuits include inverter, logic gate, adder, ring oscillator, register, and so on. In order to achieve better dynamic performance, single-threshold OFET circuit can obtain higher working speed due to the

use of p-type OFETs with better performance, simple structure and small load capacitance. For more complex digital logic circuits, it is generally preferred to use dual-gate, pseudo-CMOS, or complementary structures to obtain high noise tolerance and sufficient robustness for process disturbance. To prepare OFET devices and circuits without masks, the inkjet printing is acknowledged as a digital and on-demand way to form electrodes, functional layers (OSCs, gate dielectrics, and encapsulation), and through holes[86].

Based on the fully printed complementary structure, the nand gate, JK flip-flop, D flip-flop, and ring oscillator for clock generation were fabricated, and an RFID chip with the integration of more than 250 OFETs for enabling safe identification and ASK modulation was further designed and realized[87]. As mentioned, to take full advantage of organic electronic circuitry, it is essential to develop organic complementary circuits. Kwon and coworkers[8] were committed to improving the integration scale of the complementary structure, and enhancing the compatibility between n-type and p-type devices. The n-type and p-type OFETs are stacked in the vertical direction to achieve a three-dimensional (3D) integration (the detailed preparation procedures shown in Fig. 3a), and a 12×8 nand gate array with integration of 288 transistors was realized (Fig. 3b). Moreover, it is possible to integrate 2700 programmable OFET devices on a credit card-size (85.60×53.98 mm) base using this 3D integration. In a representative sensing system, an analog front-end circuit is required to preprocess and amplify the detected sensing signal. Operational amplifiers (OPAs) are the commonly used unit circuits in analog signal processing. They are not only used for signal amplification, but also for addition, subtraction, differentiation and integration, and signal processing functions such as filtering, voltage following, current–voltage conversion, and voltage comparison. Using OFETs to realize OPA circuit, the sensing signal can be amplified in situ at the front-end closest to the signal detection, so as to suppress the effect of noise on the subsequent signal transmission process. Considering the application of wearable ECG signal detection, an ultra-thin and flexible differential OPA circuit have been achieved based on the pseudo-CMOS structure[88]. The gain was above 200 V/V, the common mode noise rejection ratio was below -12 dB, and the SNR of the output signal was 34 dB, which could well meet the requirements of ECG signal detection. For the integration of the sensing analog front end, the full solution printing process for the OFET analog circuit will facilitate high customizability. The first-order differential OPA circuit of p-type OFETs have been prepared by inkjet printing electrode, organic semiconductor of solution process, and dielectric layer of CVD process (Fig. 3c). The resulting OPA circuit exhibited an open-loop gain of 4 under the power supply current of 100 nA. When applied to ion sensing, the signal can be amplified to improve the signal-noise ratio (SNR) of detection[89].

ROLLABLE DISPLAYS
With the development of optically transparent and mechanically flexible electronic circuitry, rollable display devices have recently gathered much interests due to their potential for enabling flexible television, e-book, video player, and portable mobile phone. The rollable displays are characterized with desirable portability, light wight, thin thickness, good foldability, low power, and wide viewing angle. E-paper display, as one representative example of rollable displays, has developed rapidly and significantly impacts our daily life. At present, researchers have devoted strenuous efforts to preparing large-scale and highly flexible displays.

Comparing with twisted-nematic liquid crystal displays, polymer-dispersed liquid crystal displays and electronic ink displays, active-matrix organic light-emitting diode (AMOLED) displays can better achieve high-resolution full-color smooth-moving images on flexible films[90]. AMOLED displays, in which the
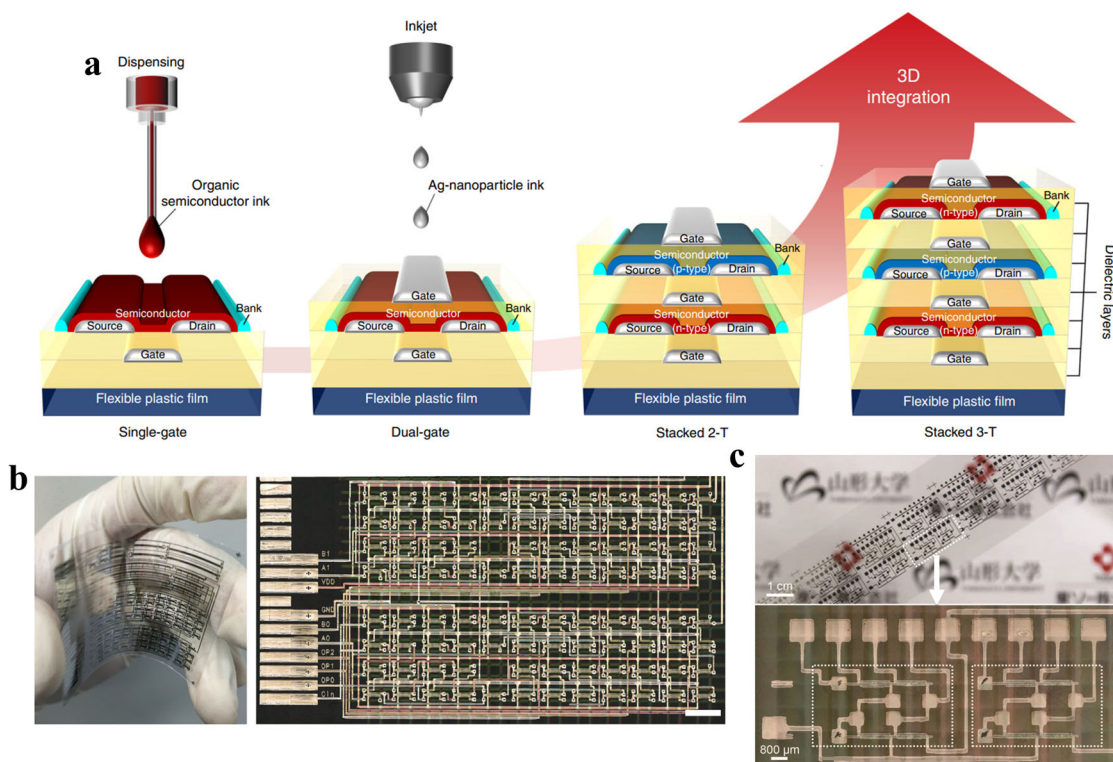
Fig. 3 The flexible signal processing circuits based on OFET circuitry. a Diagrams displaying the preparation processes of 3D monolithic integration circuits in flexible printed organic transistors. **b** Image of a large-area flexible programmable logic circuitry with a 12×8 3D NAND gate array. Reproduced with permission[8]. Copyright 2019, Springer Nature. **c** Photograph (top) and optical microscope (bottom) of the reference and amplification organic circuits. Reproduced with permission[89]. Copyright 2018, Springer Nature.

pixels are driven and switched by OFETs, possess thin, light, all-solid-state, and flexible device configurations. Meanwhile, AMOLED displays also demonstrate wide viewing angle, wide color gamut, fast respond speed, and low energy consumption[91]. AMOLEDs have been prepared based on two types of device configurations, which are top-emission configuration (Fig. 4a) and bottom-emission configuration (Fig. 4b), respectively. In the early research, AMOLEDs with bottom-emission configuration attracted some researchers due to its simple integration of OLEDs and OFETs. However, the bottom-emission requires high-transparency substrate and electrode layer, which severely restricts the selection of materials and the development of flexible AMOLEDs.

In contrast with parallel-placed bottom-emission configuration, the top-emission configuration can provide higher-resolution images and more material selection, because of the sufficient spaces induced by increasing aperture ratio between pixel OFETs and OLEDs[92]. And there are no limitations for high-transparency substrate and electrode layers[93]. However, it remains a technological challenge to prepare high-performance top-emission AMO-LEDs, which is because the multi-layer interdielectrics and interconnections inevitably result in the performance degradation of AMOLEDs[90]. Therefore, how to achieve elaborate integration of OLEDs and OFETs have always been an important research focus of top-emission AMOLEDs. Back in 2001, Huitena et al.[94] reported a pioneering work about thin-film transistor-driven active-matrix displays in the journal Nature. Their obtained AMOLEDs were furnished with 256 gray levels, which showed desirable displaying scenes. Meanwhile, the displays also exhibited comparable contrast ratio (≈8.6) to the black ink on paper. Current strategies for fabricating high-performance flexible AMOLEDs are developed primarily based on four categories: (1) improving the filed-effect characteristics (such as low V_{th} and I_{off}) of FOFETs; (2) optimizing the interfacial quality between OLEDs and OFETs; (3) developing cost-effective manufacturing processes onto the flexible substrate;

(4) increasing the amounts of pixels for AMOLEDs. For example, Yagi et al.[6] successfully prepared the world's first flexible full-color AMOLED display with a pixel resolution of 80 ppi. The fine-patterned OFETs that are integrated using an OSC separator (Fig. 4c), were employed as the flexible backplane to drive the OLED. Wherein, the OSC separator precisely pattern the active regions and interconnections, and the organic dielectrics functioning as the backplane can significantly increase the mechanical compliance of the AMOLED display. Noda et al.[95] prepared high-performance OFETs using a stable and high-mobility organic semiconductor, peri-xanthenoxanthene (PXX) derivative. Subsequently, they developed an 80-μm-thick rollable AMOLED display, in which OFETs as the gate-driver circuit were on one side. These AMOLED displays could be rolled up at a radius of 3 mm 1000 times without sacrificing the luminance and imaging quality.

The above-mentioned examples cannot satisfy the highly flexible and stretchable requirements of rollable displays. But thus far, OLEDs with high optoelectrical and mechanical performances have been reported based on some novel device assembly techniques and highly flexible materials, which will pave the way for future advances in intrinsically flexible, high-quality, and cost-effective AMOLED displays. Strain-engineering design is always considered as a simple approach to enhance the strain-tolerance capacity of OLEDs. Yin et al.[96] developed a laser-programmable method to prepare stretchable OLEDs bearing an ordered-bulking profile. The ordered bulking afforded the devices with high mechanical stretchability and robustness (Fig. 4d). These OLEDs retained a stable luminous efficiency of 70 cd A^{-1} under 70% stretching strain, and still could function well when subjected to 100% stretching strain (Fig. 4e). Moreover, the laser-programmable method presented was compatible with most OLED preparation procedures, such as spin-coating and inkjet printing. Liang et al.[97] developed a transparent conductive electrode based on a silver nanowire (AgNW) percolation network
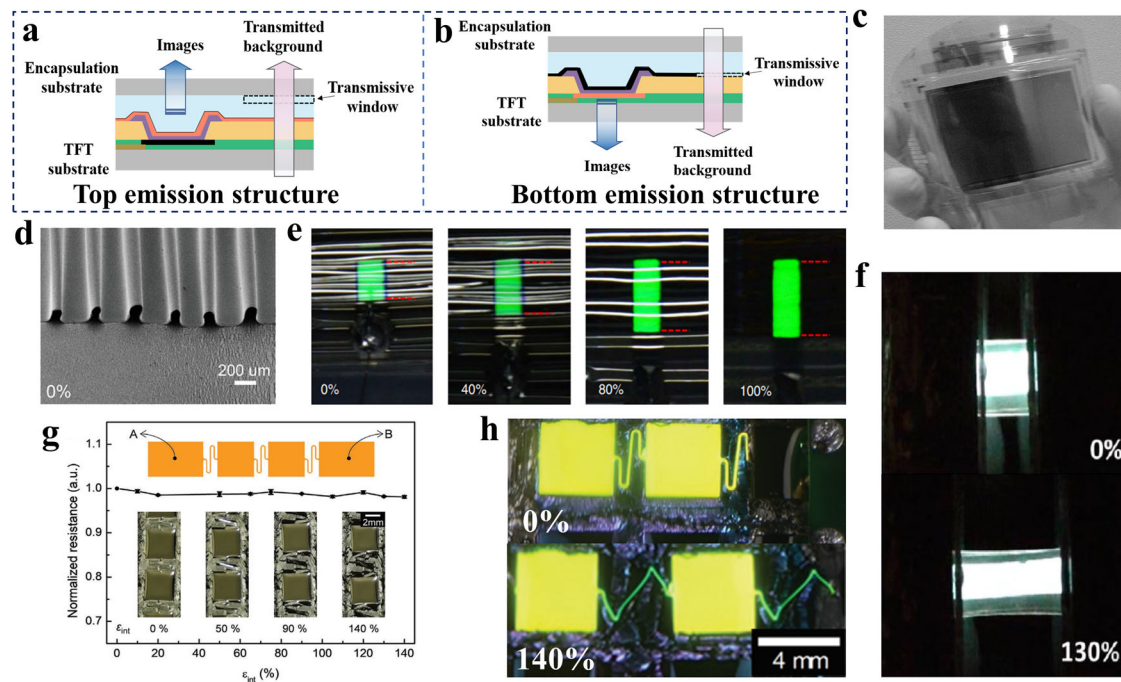
Fig. 4 Optoelectrical characteristics of flexible displays under various tensile strains. a, b The AMOLEDs with a top-emission configuration (**a**) and a bottom-emission configuration (**b**). **c** Photograph of the fine-patterned OFET backplane for the flexible AMOLED display. Reproduced with permission[6]. Copyright 2012, Wiley-VCH. **d** SEM images of stretchable OLEDs constructed by a laser-programmable buckling process. **e** Photographs of the stretchable OLEDs obtained on a 200% pre-strained substrate at 5 V under various stretching strains. Reproduced with permission[96]. Copyright 2016, Springer Nature. **f** Images of the intrinsically stretchable OLEDs at an applied voltage of 14 V under 0% (top) and 130% (bottom) tensile strains. Reproduced with permission[97]. Copyright 2014, American Chemical Society. **g** Normalized resistance of stretchable OLEDs based on a hybrid platform under stretching from 0% to 140% strain. **h** Photographs of stretchable OLEDs prepared on a hybrid platform at unstrained state and under 140% stretching strain. Reproduced with permission[98]. Copyright 2020, Wiley-VCH.

soldered with graphene oxide (Go), which exhibited high electrical conductivity, optical transmittance, and stretchability. Furthermore, they fabricated intrinsically stretchable polymer-based OLEDs using the Go-soldered AgNW network as both the anode and cathode. The obtained OLEDs could work order when subjected to 130% stretching strain (Fig. 4f) and 100 stretching-releasing cycles at 40% strain. Consequently, to obtain truly stretchable OLEDs with a stretching strain above 100% and a bending radius below 10 μm, the strain-engineering design, the preparation of intrinsically flexible material, and the improvement of interface interlayer quality all should be taken into account. In 2020, Kim et al.[98] proposed a hybrid stretchable platform comprising a bilayer architecture and an array of rigid islands. The array of rigid islands on top of the bilayer elastomeric substrate were formed and connected by a serpentine interconnecting configuration. In the bilayer architecture, the bottom PDMS substrate determined the overall flexibility and stretchability of the OLED device, and the top Silbione layer with an ultralow Young's modulus of about 0.9 kPa produced an obvious stress-relieving effect. Based on these advantages, the prepared OLEDs could be stretched up to 140% strain with insignificant change in the sheet resistance (Fig. 4g) and luminance (Fig. 4h).

BENDABLE SMART CARDS

As another reality application of OFET circuits, smart card is a generic term for a plastic card with embedded microchips. Smart cards are widely applied in identity recognition, payment instrument, encryption/decryption, personal financial record, medical record, and access control. In recent years, bendable smart cards with light weight, good adhesion, portability, high memory capacity, high confidentiality, and low cost have been paid close attention by the industry and the academia. Radio

frequency identification (RFID) tags, a representative smart card, are the simplest form of ubiquitous sensor networks to displace the existing barcode technology[99]. RFID tags can be attached to any location of an object to acquire the object information or the surrounding environment. RFID tags show great potential applications in supply-chain monitoring, logistics, anticounterfeiting, inventory controlling, pet identification, and healthcare, which is attributed to their unique benefits such as contactless identification, high data-storage capability, and desirable remote and automatic reading[100].

In general, passive RFID systems are composed of a reader and many passive tags, where an identification tag contains an antenna and a circuit. The working mechanism of passive RFID tags is depicted as follows: a reader sends out the required information to the tags. When receiving the information, all or some tags transmit their codes to the reader by extracting and modulating power from the electromagnetic field of this reader. Subsequently, these codes are sensed and decoded by this reader. It is noteworthy that when many tags response to a reader, their codes will collide in the RF communication channel, and cannot be correctly decoded by this reader. Thus, to correctly identify this tag, the use of a few tags or an anti-collision algorithm is more efficient for many practical applications[101].

In the future, all the goods should be furnished with their own RFID tags. Thus, a critical problem is the reduction of the tag cost (<1 US dollar) to satisfy a ubiquitous tag society. The use of organic semiconductor and roll-to-roll (R2R) processing techniques can enable low-cost, large-area, flexible RFID tags. Jung et al.[102] employed an all-printed and R2R-printable strategy to construct a 13.56-MHz-operated 1-bit RF tag on a plastic foil. The obtained 1-bit RFID tag not only has a low cost of approximately 0.03 dollar per unit, but also demonstrates a high clock signal up to 102.8 Hz upon the code approaching the reader. Based on the

R2R printing technology, the 16-bit and 96-bit RFID tags were achieved as well. Moreover, Yang et al.[103] also employed an inkjet-printing technology to construct a RFID tag on a paper substrate. Fiore and coworkers[87] made an important contribution to the integration of RFID tags. They, for the first time, prepared an integrated 13.56-MHz RFID tag with more than 250 transistors on a flexible foil substrate based on a printed organic complementary thin-film transistor technology. The obtained integrated RFID tags exhibited a wide reading range of 2–5 cm and a high bit-rate up to 50 bit s^{-1}. Although the achievements are far from the practical application of RF tags, the reported materials and techniques open up brand-new paths for low-cost and highly flexible RFID taps.

CONFORMABLE SENSOR AND ITS ARRAY

Conformable sensors have recently gathered much interests due to their potential for enabling personal healthcare, human activity monitoring, electronic skin, and human–machine interface[104]. Conformable sensors require high flexibility and stretchability, and they can seamlessly adhere to irregular, pliable, and locomotive objects. The conformal contact greatly depends on the stiffness and adhesion energy of a sensing device. The detailed conformal mechanics have been addressed by the Yang's group[105]. Compared with two-terminal-based sensors, the OFET-based sensors exhibit higher specificity and sensitivity. This is due to the adjustable non-covalent interaction (such as hydrogen bonds, van der Waals interaction, dipole–dipole interaction) of organic semiconductors, and the unique signal amplification and tuning capacity of OEFT configuration[106]. The acceptable sensing mechanism of OFET-based sensors is expressed as follows: when the analyte is in contact with the organic semiconductor layer, more charges in the active channel are generated and a higher drain current is induced due to the interaction or reaction between analytes and organic semiconductors. Moreover, the I_{DS} of a sensor can also be magnified under the applied V_G. Both the processes enhance the readable or recordable response signal of OFET-based sensors[4]. The sensing performance of a sensor can be evaluated by comprehensively analyzing its sensitivity, specificity, stability, and reproducibility.

Current strategies for fabricating high-performance OFET-based sensors are developed primarily in terms of four categories[107]. The first category is the most straightforward approach to synthesizing a novel multi-functional organic semiconductor with excellent charge-transportation capacity and high specific-sensing performance. The introduction of functional backbone or side-chain groups to induce the interaction or reaction with analytes can enable this goal. However, the exotic groups easily result in a noticeable reduction of field-effect performance for OFET-based sensors. The second category is to incorporate an additional functional receptor into organic semiconductors to improve the sensitivity of an OFET-based sensor while retaining its original field-effect performance. There exist three types of architectures, that are semiconductor/receptor layer-heterojunction (LHJ) architecture, semiconductor/receptor bulk-heterojunction (BHJ) architecture, and semiconductor layer interface-located receptor assembly. For example, Huang et al.[108] employed a tris-(penta-fluorophenyl)borane (TPFB) CuPc/CoPc BHJ architecture to prepare a OFET-based sensor, which displayed ultrahigh sensitivity to NH$_3$ (limit of detection ≈ 350 ppb) due to the strong hydrogen interaction between NH$_3$ and TPFB. The third category is to downscale the thickness of the organic semiconductor layer. It is acknowledged that to ensure the high field-effect performance of OEFTs, the organic semiconductor layer should be possessed with a high film thickness of approximately several tens of nanometers. However, the high semiconductor film thickness severely restricts the diffusion of analyte molecules across the active layer and degrades the interaction between analytes and semiconductors.

Therefore, the exposure of the conductive channel of ultra-thin organic semiconductor film is more beneficial for improving the sensitivity and response speed of OFET-based sensors compared to the thick semiconductor film[109]. As a representative example, Li et al.[110] developed an ultra-thin dendritic-microstripe semiconductor film with 4–6 molecular layers based on the dip-coating approach. The obtained OFET-based sensor demonstrated a higher sensitivity to NH$_3$ and a shorter response/recovery compared to the thick film-based devices. This was due to the one-dimensional continuous, micro-structured and ultra-thin nature of the low-dimensional semiconductor films. The fourth category is to optimize the device architecture. As mentioned, different sensing applications require different device configurations. For example, the BG configuration is more appropriate for the gas sensor due to the exposure and better contact between gas analytes and semiconductor layer. The suspended gate structure with an air gap as the dielectric provides higher sensitivity to pressure[111]. In addition, various components (gate electrode, dielectric, semiconductor, S/D electrodes) and interfacial quality are also critical factors to improve the sensing performance of OFET-based sensors. Details and special examples have been reviewed by Zhu's group[107]. To meet the practical demands, the majority of conformable sensors (such as pressure, temperature, stress, gas, chemical, biological, photonic, and memory sensors) reported thus far have shown ideal sensing performance and high flexibility. In this review, we will briefly introduce several commonly used flexible sensors.

Biological sensors

Biological sensors can convert biochemical signals into electronic signals. Biosensors for sensing various biological substances (such as DNA, protein, glucose) and biological signals (such as blood pressure, nerve impulse, wrist pulse, cell behavior) have shown great potential for achieving health monitoring, cell controlling, and drug delivery. The realization of biosensors that work order under various large mechanical deformations is important for the next-generation smart wearable electronic applications. High-performance biosensors are characterized by high sensitivity, excellent specificity, desirable biocompatibility, and high flexibility. Currently, the advances on OFETs for biological sensing have lagged behind the OECTs, which is because OECTs have better work stability in an aqueous environment, lower operation voltage, and unique label-free detection[4]. It is acknowledged that an aqueous environment is essential for human body. Thus, the first concern is to reduce the effects of aqueous solution on OFET-based biosensors. To achieve this goal, Yan et al.[112] reported an ion-sensitive field-effect transistors (ISFETs) on inexpensive disposable substrates like glass and plastics. The ISFETs were fabricated with an extended gate structure and a PECVD Si$_3$N$_4$ layer as the pH-sensitive area, which displayed outstanding stability and durability due to the electrical and chemical isolation induced by the extended gate structure. Their obtained ISFETs also demonstrated superior operation stability and nearly ideal pH sensitivity up to 54 mV pH^{-1} (Fig. 5a). This technology highlights great potential application in single-use multi-analyte biosensors.

Glucose is an essential monosaccharide in human blood, and significantly impacts the metabolic homeostasis. Hypoglycemia and diabetes are the two most common blood sugar-related chronic diseases. Therefore, enabling the real-time monitoring of the blood sugar is cardinal significance for human health[111]. To enable the highly sensitive and stable glucose detection of OFET-based biosensors, the separation of the detection area and the working area, as well as the use of gate electrodes as the sensing area, are two efficient strategies[113]. Elkington et al.[114] prepared a top-gated P3HT-based OFETs using a Nafion film as the gate electrodes. The Nafion film has a sensing enzyme glucose oxidase. The polymeric membrane materials function as the recognition
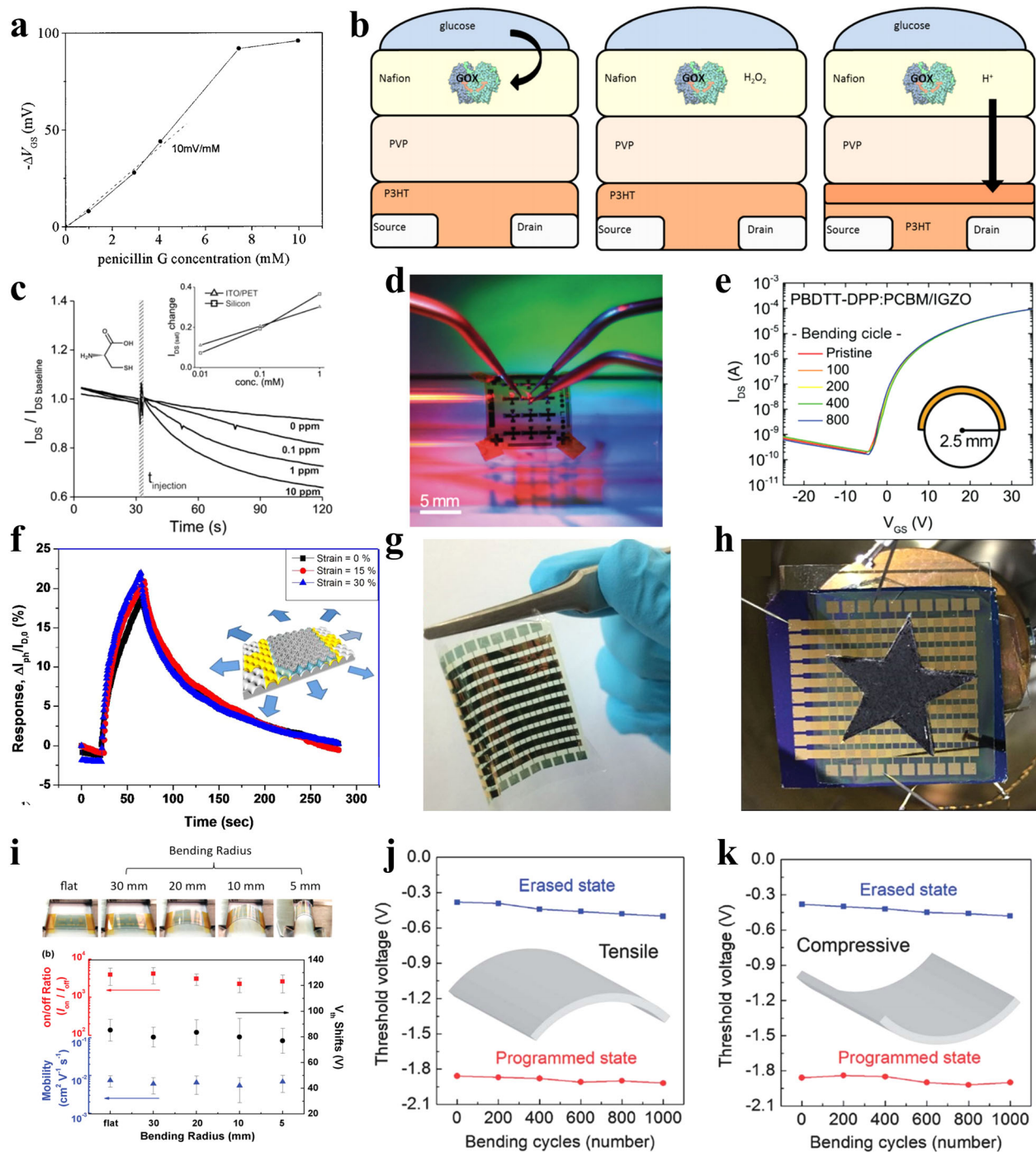
Fig. 5 Detection sensitivity and strain-tolerance of flexible biosensors, photosensors, and memories. a Gate voltage shift (ΔV_{GS}) as a function of gas concentration for the ion-sensitive field-effect transistors. Reproduced with permission[112]. Copyright 2005, American Institute of Physics. **b** The sensing mechanism of the OFET-based sensor for the detection of glucose. Reproduced with permission[114]. Copyright 2014, American Institute of Physics. **c** Detection sensitivity of the FOFET-based biosensors when exposed to the cysteine solutions with various concentrations. Reproduced with permission[116]. Copyright 2009, Elsevier. **d** Photograph of a flexible phototransistor placed on the curved surface with a bending radius of 5 mm. **e** Transfer characteristics of the flexible transistors when subjected to multiple bending cycles at a bending radius of 5 mm. Reproduced with permission[120]. Copyright 2015, Wiley-VCH. **f** The time-dependent photoresponse of stretchable photodetectors with an organic−inorganic heterojunction under a multiaxial stretching strain of 0−30% ($V_D = 1$ V, $P = 1.42$ mW cm^{-2}). Reproduced with permission[134]. Copyright 2017, American Chemical Society. **g** Photograph of a flexible phototransistor array (10 × 10). **h** Image of a flexible phototransistor array to sense a pentacle pattern. Reproduced with permission[140]. Copyright 2016, Wiley-VCH. **i** Variations of I_{on}/I_{off} ratio, V_{th} shift, and carrier mobility of the FOFET-based memory with the decreased bending radius. Reproduced with permission[157]. Copyright 2014, Wiley-VCH. **j**, **k** V_{th} of the low-power flexible memory arrays at the programmed and erased states under multiple bending cycles with a bending radius of 9 mm. Reproduced with permission[168]. Copyright 2013, Royal Society of Chemistry.

element of glucose detection for OFET-based sensor. Their explanation for the sensing processes of the P3HT-based OFETs includes three steps: (1) the diffusion of glucose to the GOX in the Nafion matrix and the generation of H_2O_2; (2) the oxidation of H_2O_2 and the generation of protons; (3) the diffusion and activation of protons to the P3HT channel (Fig. 5b). The integrated sensors showed sensitive respond to a wide range of glucose concentrations in saliva. As another good example, Bao's group[115] developed an enzyme-free OFET-based sensor and enabled its application in chemical and biological signal detection. The OFET-based sensor was prepared with a p-type polymer 5,5′-bis-(7-docedyl-9H-fluorene-2-yl)2,2′-bithiophene (DDFTTF) as the organic semiconductor and a crosslinking poly(4-vinylphenol) (PVP) as the gate dielectric. These obtained sensors demonstrated stable and sensitive detection to glucose with low concentrations of parts per billion in aqueous solutions under a low applied voltage. These studies open up a door for lost-cost, low-voltage, aqueous-resistance and highly sensitive biosensors for detection of glucose.

The acidity and alkalinity of the human body are different from those of other living things. Each organ, blood and body fluid of human body has different healthy acidity and alkalinity. The human body has a certain capability to adjust the balance of pH values. However, once this balance is broken, the human body will be out of balance and the human health will be seriously threatened. Therefore, enabling a real-time and sensitive pH value monitoring is significant for human health. Roberts et al.[116] prepared a flexible, transparent OFET-based biological sensor with a BGTC configuration. Polymer 5,5′-bis-(7-dodecyl-9H-fluoren-2-yl) 2,2′-bithiophene (DDFTTF) was used as the organic semiconductor and patterned PEDOT:PSS was used as the S/D electrodes. A crosslinked poly(4-vinylphenol) (PVP) with 4.4′-(hexafluoroisopropylidene)diphthalic anhydride (HDA) was employed as the gate dielectric, which efficiently avoided the solvent damage to dielectric materials and decreased the operation voltage to <1 V. The obtained sensors exhibited high sensitivity to cysteine (LOD ≈ 100 ppb), 2,4,6-trinitrobenzene (LOD ≈ 100 ppb) (Fig. 5c) and pH value (pH 3–11). Moreover, the sensor also demonstrated low input power and good operation stability in air and water environments. This device assembly techniques take a step toward the low-cost, high-sensitivity, and multi-functional biosensors.

In addition to the above-mentioned glucose detection and pH detection, the sensing of some other biological substances and signals have also highlighted great potential for enabling implantable medical monitoring and treatment. For example, flexible OFET-based biosensors for detection of ions (such as K^+, H^+) in a human body can indirectly indicate the cardiovascular diseases[117]. Flexible OFET-based biosensors for detection of electrical stimulation can be used as the neural prostheses to simulate the human body functions[118]. However, there exist two challenges meriting further consideration: (1) the sensing stability of flexible OFET-based biosensors should be improved; (2) the integration of flexible OFET-based biosensors into complex systems for enabling multiple point of care (POC) diagnostics should be developed.

Photonic sensors

Photonic sensors can convert photons into electrical signals[39]. Phototransistors (PTs), as one significant type of optical transducers based on FET configuration, can combine the light-detection capability of photodiodes and signal-amplification function of transistors. The charge-carrier density in the active channel of PTs can be modulated by both the applied V_G and incident light illumination[119,120]. In contrast with other photosensors such as photodiodes and photoconductors, PTs show higher light sensitivity, lower noise level, and highly tunable photosensing performance, and they can be readily integrated into the

electronic circuitry due to their CMOS-like configuration[121]. Moreover, organic PTs (OPTs) are characterized with inherent compliance, light weight, good compatibility with a flexible substrate, large-area, and low-temperature solution manufacturing[122]. These advantages together make them a promising candidate for medical imaging, optical communications, artificial retina, remote control, night surveillance, and biological health monitoring[3,105].

In general, the operation mechanism of OPTs can be explained by four physical processes, that are photo-exciton generation, exciton dissociation, hole transport, and electron trapping, respectively (for a p-channel device)[123,124]. The photocurrent induced by light illumination was primarily on basis of the generation of electron–hole pairs and the shift of V_{th}[125]. Specifically, when the OPTs operate in the accumulation ($V_g <$ V_{th} for a p-channel device), the photovoltaic effect is dominant, whereas when the OPTs operate in the depletion ($V_g > V_{th}$), the photoconductive is dominant[126]. The photosensing performance of OPTs is determined with regard to a comprehensive consideration of photocurrent (I_{photo}), photocurrent/dark current (I_{light}/I_{dark}) ratio, photosensitivity (P), photoresponsivity (R), detectivity (D^*), and external quantum efficiency (EQE).

In the past few years, the photosensing performance of OPTs were improved by developing highly sensitive photoactive layer materials, optimizing device configurations and designing interfacial engineering[119]. Among them, organic photoactive layer materials are directly correlative with the sensing performance of OPTs. These photoactive materials are classified into single-component photoresponse materials (small molecules and conjugated polymers), heterojunctions (layer- and bulk-heterojunction), and D–A cocrystals (or copolymers). As mentioned, comparing with organic small molecules, polymers are more suitable for flexible electronics[127]. Organic small molecules (such as pentacene, DNTT, C8-BTBT) are extensively employed in rigid photodetectors due to high carrier mobility and certain light sensitivity, but the high-crystallinity nature seriously restricts their use in flexible and stretchable OPTs. The application of organic small molecules in OPTs have been summarized in detail by Hu's group[119]. For polymer semiconductors, high exciton binding energy (0.2–1 eV) limits their application in OPTs. Therefore, it remains a considerable challenge to simultaneously improve the carrier mobility, photosensitivity and flexibility of polymer semiconductors. Next, we will summarize the reported strategies to achieve this goal.

The first strategy is to prepare novel donor–acceptor (D–A)-conjugated polymers with strong photosensitive capability due to the low bandgap. Regulating the amount and position of the donor and acceptor units can effectively improve the optoelectrical performance of D–A-conjugated polymers. The incorporation of the alternating electron-rich and electron-deficient units is beneficial for the decrease of bandgap[128]. Liu et al.[129] synthesized a D–A-conjugated polymer PFTBT by the Suzuki coupling polymerization, and further prepared high-quality, large-scale PFTBT nanowires using a template dipping method. The polymer nanowires are amorphous and flexible, and possess good photosensitivity and reliable reproducibility. Zhu et al.[130] synthesized a single-component D–A-conjugated polymer (PBIBDF-TT), which displayed obvious ambipolar characteristics and sensitive photoresponse to NIR illumination. These two research results also indicated that the polymer NWs could afford OPTs with higher photosensing performance compared with their thin-film counterparts. This is because large surface-to-volume of polymer NWs easily form more trap sites, thereby facilitating the injection of photo-induced carriers.

The second strategy is to form p–n junction in the BHJ structure. The p–n junction consists of donor molecules and acceptor molecules[131]. Under light illumination, the photo-induced excitons diffuse to the D/A interface, followed by the exciton dissociation

into holes and electrons. Subsequently, the holes accumulate in the HOMO of the donor, while the electrons accumulate in the LUMO of the acceptor. Yang's group[120] prepared an organic BHJ by combining low bandgap-conjugated polymer poly[2,6'-4,8-di(5-ethylhexylthienyl)benzo[1,2-b;3,4-b]dithiophene-alt-5-dibutyloctyl-3,6-bis(5-bromothiophen-2-yl)pyrrolo[3,4-c]pyrrole-1,4-dione] (PBDTT-DPP) and [6,6]-phenyl C61 butyric acid methyl ester ($PC_{61}BM$). Polymer PBDTT-DPP and $PC_{61}BM$ were employed as the electron donor and electron acceptor, respectively. The resulting BHJ displayed broad harvesting of UV and NIR photons with a high detectivity up to 10^{12} Jones. Moreover, the devices sustained 800 bending cycles at a bending radius of 2.5 mm with minimal degradation of optoelectrical properties (Fig. 5d, e).

The third strategy is to construct a LHJ structure by preparing the photosensitive layer on the top/bottom of the organic semiconductor layer. The working mechanism of the LHJ structure (for a p-type device) is interpreted as follows: under light illumination, majority of excitons are instantaneously generated in the photosensitive layer, followed by approaching the photosensitive-semiconductor layer interface, and are rapidly dissociated into holes and electrons. Holes incline to diffuse to the semiconductor layer, whereas electrons squint towards accumulation in the photosensitive layer owing to the shallow valence band and high electron injection barrier between photosensitive and semiconductor layer. Consequently, the increasing amounts of holes in the active channel will substantially lower the effective barrier height and facilitate the charge tunneling and transportation, thereby enhancing the photocurrent[132,133]. Trung et al.[134] constructed an organic-inorganic LHJ structure by fabricating free-standing ZnO nanorods onto the PEDOT:PSS transporting layer. The LHJ showed highly sensitive respond to UV illumination due to both photovoltage and photogating effects. Subsequently, an LHJ-based phototransistor was prepared on a 3D micropatterned stretchable substrate with plenty of bumps and valleys, which could still remain good electrical properties when subjected to uniaxial and multiaxial strains of 30% for 15,000 stretching cycles (Fig. 5f). Furthermore, these devices also demonstrated potential wearability and desirable photodetection capability on the human body. In 2020, our groups[135] prepared an intrinsically stretchable organic phototransistors (STOPTs) based on a LHJ of hybrid polymer semiconductor and C60. The obtained STOPTs exhibited a high photosensitivity of ~1500, and could endure high stretching strain up to 100% with little sacrifice of photosensitivity. It is worth noting that perovskites have recently been extensively used as the photosensitive layer materials for photosensors. Currently reported phototransistors based on perovskite/organic semiconductor LHJ architecture showed superb photosensing performance, such as DNTT/CPB QD LHJ[123] and DPP-DTT/CPI QD LHJ[124]. However, it is difficult to pioneer the application of perovskites into highly flexible phototransistors due to their high-crystallinity nature.

In addition to the modification of photosensitive layer, optimizing the device configuration (such as dual-gate[136], short channel[137], and vertical device configuration[138]) and interfacial quality (such as electrode-semiconductor layer interface[139]) are also seen as two efficient strategies to improve the photosensing performance of flexible OPTs. In term of the reported high-performance OPTs, enabling the transistor array is imperative for the flexible image-sensor application. Huang's group[140] used polylactide (PLA) as the gate dielectric and DNTT as the organic semiconductor to construct a photosensitive and flexible OPT. The interface charge-trapping effect between PLA and DNTT afforded the OPTs with high photosensitivity up to 10^4. Furthermore, they successfully incorporated the device into a 10×10 phototransistor array to sense a pentacle pattern (Fig. 5g) and achieved a high-resolution imaging for a star-shaped object (Fig. 5h). The same year, Lee et al.[141] also reported a 10 × 10 phototransistor array for

use as highly flexible image-sensors with high-resolution 2D spatial response to incident photonic signals.

Memory sensors

Memory, as a fundamental component of future electronic computing systems, is responsible for data processing, storage, and communication. Developing highly flexible, high-density, low-voltage, and non-volatile memories are the future goal. Nevertheless, currently reported inorganic memories are irreconcilable with flexible substrates. Based on these reasons, OFET-based memories stand out because of their unique advantages with low cost, light weight, non-destructive readout, high data-storage density, structural flexibility and multi-bit storage in a single cell as well as overall integration compatibility with complementary logic circuits[142,143]. In terms of the charge storage and polarization of the gate dielectrics, the OFET-based memories are generally classified into three categories, viz., floating-gate transistor memory, charge-trapping transistor memory, and ferroelectric transistor memory[144]. To satisfy the requirement of product wearability, miniaturization and high density, several memory parameters such as memory window, retention, endurance, flexibility, and integration need to be taken into account.

Floating-gate transistor memory (FGTM) is the most common type of non-volatile memory because of the non-destructive readout and direct integration in transistor-based circuits. For FGTM, the charge carriers from the active channel are preserved in the floating-gate layer under programming operation by applying an external bias on the gate electrode. Moreover, the preserved charge carriers in the floating-gate layer are removed back to the active channel layer under erasing operation by applying a reverse bias on the gate electrode. The preservation and removal of charge carriers in the floating-gate layer determines the channel conductance and thereby manipulates the V_{th}. Accordingly, the change in V_{th} and I_{DS} can be used to evaluate the memory performance of the FGTM[145]. Considering the FGTM architecture, the floating-gate layer and the (blocking and tunneling) dielectric layer significantly impact the charge-retention time and programming/erasing speed.

To obtain high-speed, long-term-retention, and low-energy-consumption flexible FGTMs, choosing suitable floating-gate materials with desirable mechanical compliance, high dielectric constant, and defect-free interface is of crucial importance. At present, the reported floating-gate materials mainly contain the following four types. The first type is the conventional metal (such as gold (Au), copper (Cu), aluminum (Al)) film, and metal nanoparticles (such as Au NPs, Ag NPs)[146]. However, the unavoidable penetration of metal atoms into the gate dielectric layer during high-vacuum vapor deposition easily causes large charge leakage, low coupling ratio, and inferior charge-retention. Meanwhile, the thickness-dependent film quality, as well as the uncontrollable particle size and spacing, largely degrade the memory performance[147,148]. The alternate charge-storage elements with high binding energy and large-area density can effectively regulate the self-assembly behavior and film morphology of metal nanoparticles, thus reducing the number of charge tunneling between nanoparticles. Semiconducting nano-floating gate (such as C60, rGO, and SWCNTs), as the second type of floating-gate material, have attracted people's attention. Unlike conventional metallic floating gate, the semiconducting nano-floating gate provides adjustable charge-trapping capacity, tunable functional memory characteristics, and good compatibility with large-area printing techniques for enabling multi-functional flexible FGTMs[149]. But it is imperative to develop convenient solution-processing methods to fabricating high-quality semiconducting nano-floating-gate materials. The third type is based on the separated molecular microdomains induced by phase separation. To fabricate high-quality separated molecular microdomains,

Wu et al.[150] attempted to blend poly(styrene) (PS) with 6,13-bis (triisopropylsilylethynyl)pentacene (TIPS-Pen) in a solution. During spin-coating, TIPS-Pen tends to aggregate and form plenty of evenly distributed separated microdomains in the PS matrix. With separated microdomains as the charge-trapping sites, their prepared FGTMs exhibited large memory window (≈26 V), low reading voltage (≈0 V), high memory on/off ratio (>3500), reliable P/E switching endurance (>500 cycles) and long charge-storage retention time (>5000 s). The fourth type is to take advantage of the synergistic effect of various floating-gate materials, such as hybrid layer-heterojunction (CuPc/N-C$_{60}$[151], rGO sheets/Au NPs[152]) and core-shell structure (Au NP-SiO$_2$ complexes[153]). This strategy can integrate the advantages of various floating-gate materials, and provide superior memory performance to single floating-gate material.

Charge-trapping transistor memory (CTTM) requires an electret layer to adjust the charge density of the active channel[154]. An electret is an insulating dielectric material with quasi-permanent electrical charges or dipolar polarization[142]. Unlike FGTMs, the electrical charges can be permanently stored in the electret layer of CTTMs during memory operation. Although the charge trapping is detrimental for the carrier transport of an OFET, it is conducive to enable the memory behavior in a simpler approach comparing with the floating gate[155]. CTTMs exhibit high data-storage density, long retention time, good operation reliability, quick P/E speed, and desirable integration compatibility[145]. Among electret materials, polymer electrets show greater potential for achieving flexible, non-volatile OFET-based memories due to their cost-effective solution processing, low-temperature manufacturing, and good compatibility with a flexible substrate. Meanwhile, the mechanical and physical characteristics of polymer electrets can be controlled by optimizing the polymer molecular structure such as side-chain moieties and π-conjugation length. Therefore, the physical characteristics of polymer electrets, including hydrophobicity, polarity, dielectric constant, surface morphology, and interface barrier energy, produce a decisive effect on the memory performance of CTTMs[143,156].

At present, commonly used polymer electrets are classified into three categories: (1) non-polar hydrophobic polymer electrets, such as PS, poly(2-vinynaphthalene) (PVN), poly(4-methylstyrene) (P4MS), and PaMS; (2) polar hydrophilic polymer electrets, such as poly(vinyl alcohol) (PVA), poly(2-vinylpyridine) (PVPyr), and poly(4-vinylphenol) (PVP); (3) bilayer polymer electrets, such as PS/poly(vinylidenefluoridetrifluoroethylene) (P(VDF-TrFE)) and PVN/P(VDF-TrFE). Baeg et al.[142] systematically explored the effects of hydrophobicity and polarity of polymer electrets on the memory performance of OFET-based CTTMs. They found that the non-polar and hydrophobic nature was beneficial for achieving efficient charge trapping and improving memory behavior. This is because non-polar and hydrophobic polymer electrets could form strong interaction with organic semiconductor. However, non-polar and hydrophobic polymer electrets easily caused a rapid dissipation of transferred charges from the conductive channels due to the negative effects of dipoles, residual moisture, or ions. Yu et al.[157] employed polyimide (PI) electrets with identical electron donor and different building blocks to explore the charge-transfer effects on the memory behavior of multi-level non-volatile CTTMs. The results indicated that the memory device with strong electron-donating capacity showed only hole-trapping behavior, whereas the ones with relatively weak electron-donating capacity exhibited ideal programmable flash-type characteristics. Furthermore, they prepared flexible CTTMs with multileveled memory behavior, which displayed reliable memory performance even when bent to a small curvature radius of 5 mm (Fig. 5i).

Ferroelectric transistor memory (FETM) using ferroelectric layers as the gate insulators has been extensively explored. The FETMs show high programming speed, non-destructive speed, long data retention, low-operation voltage, and scalable feature size

(≈4F^2)[158,159]. Ferroelectric is referred as the spontaneous electric polarization of polymers or inorganic crystalline materials, and can be reversed upon suffering from the external electric stimulation. The polarization state of the ferroelectric dielectric layer can be controlled by modulating the P/E gate voltages, thereby adjusting the channel conductance of semiconductors, and enabling the memory behavior of FETMs[160]. A suitable ferroelectric material typically shows a polarized electric-field hysteresis loop, which is identical to the magnetized magnetic-field hysteresis loop for the magnetic materials. A substantial amount of inorganic perovskite materials, such as BiFeO$_3$, Pb(Zr,Ti)O$_3$, Sr(Bi,Ta)$_2$O$_9$, Pb-Zr-Ti oxide, and Hf$_{0.5}$Zr$_{0.5}$O$_2$, have been used as the ferroelectric dielectric materials due to their large spontaneous polarization, high polarization switching, low coercive field, high Curie temperature, excellent thermal stability, and available epitaxial growth[161]. However, the high-temperature growth, poor film crystallinity, and incompatibility with flexible substrate seriously restricts the application of inorganic ferroelectric materials in flexible FETMs. Moreover, their charge injection, trapping, and depolarization are readily suppressed under the depolarization field[162]. Ferroelectric polymers represented by poly(vinylidenefluoride) (PVDF) and its copolymers, are frequently applied in flexible non-volatile FETMs due to their high dielectric constant (κ ≈ 10.3), good structural pliability, large spontaneous polarization (~0.1 C m^{-2}), high polarization stability, desirable switching speed, and convenient solution processability[163,164]. In addition, the strong –C–F– dipolar polarization in the β-crystalline phase significantly increases the bias hysteresis of ferroelectric polymers[165].

P(VDF-TrFE), as one of PVDF derivatives, is fabricated by incorporating TrEE side groups in the PVDF molecular chains. The induced steric effect is advantageous to form a full *cis*-conformation and crystallize into the β-phase[166]. The P(VDF-TrFE) not only has better memory performance than the PVDF, but also exhibits desirable low-temperature solution processing and good compatibility with flexible/stretchable substrate. Hwang et al.[158] reported a flexible multileveled non-volatile FETMs by employing a ferroelectric polymer PVDF-TrFE as the gate dielectric. Each level of the prepared FETMs showed a long data retention over 10^5 s and a repeated P/E endurance over 10^2 cycles. Moreover, these devices could sustain small bending radius of 5.8 mm and multiple bending cycles more than 1000 with minimal degradation of memory performance. However, currently reported FETMs based on P(VDF-TrFE) as the ferroelectric dielectric layer usually showed high operation voltage (30–100 V) due to high coercive field and high dielectric film thickness[163,167]. To address this issue, Xu et al.[160] developed a low-operation-voltage flexible FETM using double-layer ultra-thin AlO$_x$ films to sandwich an ultra-thin ferroelectric polymer P(VDF-TrFE-CTFE) film. The obtained flexible FETMs showed super memory performance with a high carrier mobility up to 3.3 cm^2 V^{-1} s^{-1}, a reliable memory switching endurance over 2700 cycles, a high data-retention capability over 80,000 s, a high memory on-off ratio over 100, and a record-low-operation voltage of only 4 V. Meanwhile, these devices could retain relatively stable memory performance when subjected to a bending radius of 5.5 mm for 750 bending cycles.

For stretchable OFETs, the stretching strain significantly impact their field-effect performance. Therefore, the effects of mechanical deformations on the memory performance merit further attention. Zhou and co-workers[168] established a qualitative relation between bending behavior and electrical characteristics of a flexible memory transistor. Under the programming process, the tensile strain induced the V_{th} to shift to a negative direction, whereas the compressive strain induced the V_{th} to shift to a positive direction (Fig. 5j, k). This is attributed to the decreased carrier mobility and dielectric thickness under tensile strain, and the increased carrier mobility and dielectric thickness under compressive strain. Taking a step forward, Hu's groups[169] prepared high-performance flexible FGTMs with a vertical device architecture, which displayed much

higher memory performances than conventional planar FGTMs. The ultrashort channel length reduced the carrier migration distance and degraded the effects of the grain boundary and defects on the carrier transmission, thereby ensuring high driving capability and operating speed. Meanwhile, they also found that the vertical architecture has better mechanical stability compared with their planar counterparts, attributing to the reason why the carrier transmission along the channel direction is less influenced by the cracks and dislocation formed during mechanical bending deformations. Consequently, comparing with memory transistors with a planar architecture, the ones with a vertical architecture possess much higher mechanical stability and memory performance.

ARTIFICIAL SKIN

Human skin, the biggest organ of a human being, plays a significant role in shaping our connections with the outside environments. Skin is composed of many integrated sensors, which can effectively feel various external stimuli and make an instant respond[170]. Specifically, upon suffering from various external stimuli, the highly specialized sensing receptors in human skin can instantaneously transduce external stimuli into electrical signals, and then send the electrical signals to the central nervous systems for further identification and processing. Lastly, the collected signals are interpreted by the somatosensory cortex. As such, people are able to keep healthy and safe activities in a complex environment[171]. Inspired by human skin, artificial skin (also termed as sensitive skin, smart skin, or e-skin) has recently attracted considerable attention from the medicine and the academia, attributed to their similar physical characteristics to human skin and higher sensory capabilities. These artificial intelligent e-skins with multiple sensing modules can simultaneously respond to various external stimuli and signals, such as impedance, pressure, temperature, humidity, strain, twisting, and imaging[172]. Moreover, ideal artificial skin is also able to continuously and efficiently monitor the biopotentials of the human body irrespective of time and location for ensuring an earlier and accurate disease diagnosis. The history, design consideration, and recent progress of artificial skin have been reviewed by Bao and coworkers[173,174].

Artificial skin with human-like sensory capabilities is unleashing a potential for enabling medical diagnostics, autonomous intelligent robots, and biomimetic prosthetics. The design and synthesis of functional materials, as well as the development of device assembly techniques for high-performance artificial skin have been carefully summarized[173]. To imitate or even surpass the functionalities of human skin, the following performance benchmarks for evaluating artificial skins should be comprehensively addressed.

Flexibility and stretchability

Good flexibility and stretchability are of crucial importance to retain stable sensory capabilities of artificial skin under various complex mechanical deformations, such as bending, stretching, compressing, and twisting. It is acknowledged that 20%–30% stretching strain is enough for the most practical applications of artificial skins. Thus, developing a sensing system bearing a bending radius below 2 mm and bearing a stretching strain above 30% is highly desirable for artificial skin.

Sensory specificity and sensitivity

The specificity can help a sensing system to correctly detect the target analyte from all the interferent analytes in the environment. For example, Lee and coworkers[175] reported a textile-based pressure sensor based on rubbery dielectric-coated highly conductive fibers, which was afforded with ultrahigh sensitivity,

superior mechanical durability and fast response speed. Moreover, their prepared four textile-based pressure sensors worn on the fingers of the glove could exactly control the motion behavior of a quad-rotor aircraft (Fig. 6a). High sensitivity can facilitate the sensing system to precisely and quickly detect the target analytes with low concentration or sense the external stimuli with runt pulse, so as to prevent the stimuli damage to human health.

Adhesion and conformability

To improve the sensing accuracy of skin-like electronics, they should have good adhesion, and can adhere seamlessly to irregular, pliable, and locomotive objects[1]. For example, the skin-like OFETs, prepared by Bao's group[26], could be seamlessly attached on the back of the human hand (Fig. 6b).

Easy integration

Like human skins, the artificial skins should have an ability to discriminate various bio-signals and physical stimuli from the surrounding environment. Thus, multi-functional smart e-skin with diverse sensory modules is the future research focus (Fig. 6c)[176]. However, to enable high-resolution sensing, each device should be efficiently connected. Kim and coworkers[177] constructed a prosthetic artificial skin to sense multiple external stimuli, including temperature, humidity, strain, and pressure.

Low-cost and large-area manufacturing

Low-cost and high-density sensory array is a prerequisite for commercialization and application of intelligent artificial skin and wearable electronics. Some researchers have been committed to preparing high-density flexible sensory array. For example, Pei and coworkers[178] reported fully printed 10×6 flexible transistor arrays based on their developed water-based silver-nanowires screen-printed ink and high-resolution printed patterns of AgNWs on the PET substrate. The obtained transistor could be worn on a finger (Fig. 6d). Bao's group[179] constructed a stretchable and low-voltage synaptic transistor array with a device density of 20 device cm^{-2} based on the inkjet-printed method (Fig. 6e). Taking a ground-breaking step, they developed an intrinsically stretchable transistor array with an unprecedented device density of 347 transistors per square centimeter, and could endure high stretching strain up to 100% and multiple stretching cycles of 1000 with minimal degradation of carrier mobility[81]. These studies illustrated that the obtained high-density transistor array could be employed as a backplane for high-resolution touch sensing in the conformal e-skin.

Self-healing

Like human skin, artificial skins should also have an ability to repair its initial appearance and nearly original sensing capabilities after suffering from external damage[180]. At present, various self-healing materials have been successfully fabricated based on the introduction of healing agents and the incorporation of dynamic reversible bonds[181]. Both the strategies can induce the energy dissipation in polymers through bond breakage when subjected to stretching strain, while maintaining the original charge transport capability. Bao's group[16] reported a supramolecular PDMS–MPU$_x$-IU$_{1-x}$ polymer film with notch-insensitive high stretchability (1200%) and autonomous self-healing even in artificial sweat (Fig. 6f). This was mainly due to the incorporation of a mixture of strong and weak dynamic crosslinking hydrogen bonds into the elastomer matrix. Based on this self-healing polymer film, they further prepared a 7×7 strain sensor array to precisely sense the mechanical deformations caused by external stimuli (Fig. 6g). Years later, Oh and coworkers[18] incorporated chemical moieties into the conjugated polymers to increase the amorphous fraction and decrease the relative crystallinity, thereby
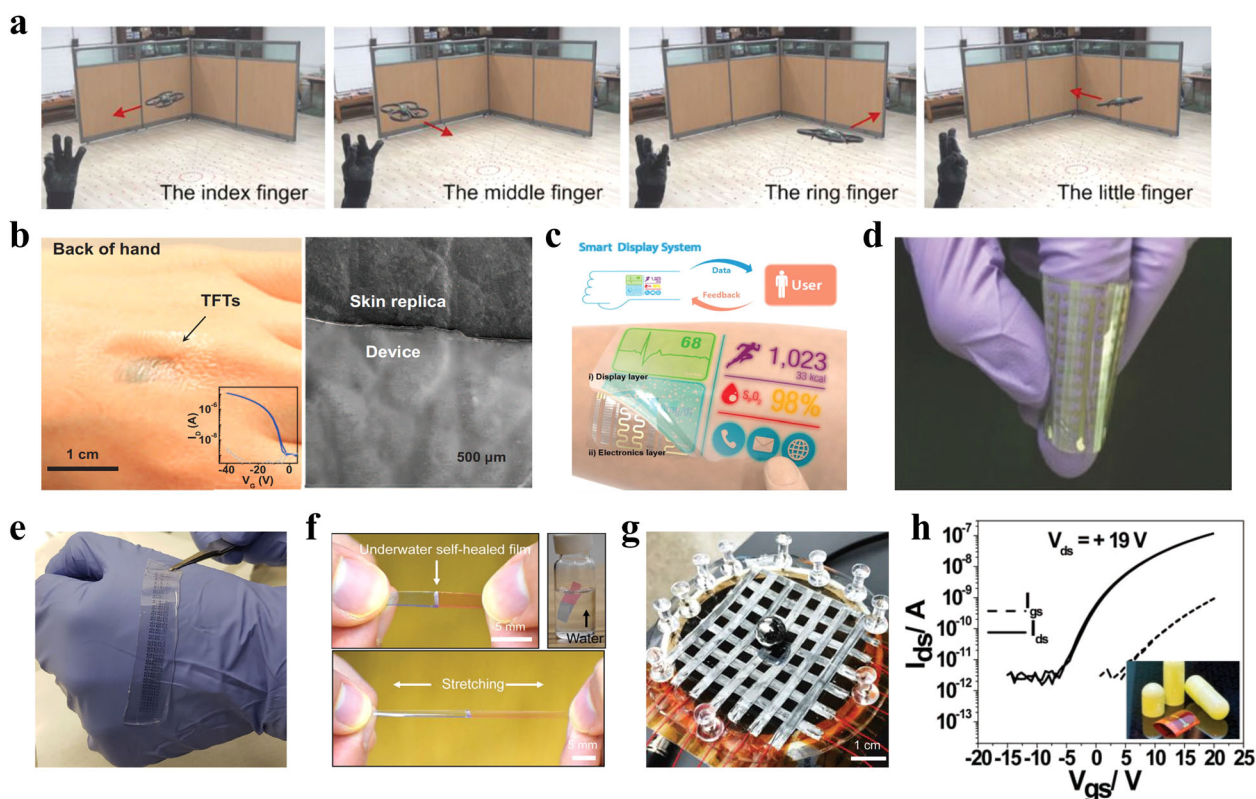
Fig. 6 Multi-functional characteristics of artificial skin. a Photographs showing the remote controlling of a quad-rotor aircraft by the textile-based pressure sensors. Reproduced with permission[175]. Copyright 2015, Wiley-VCH. **b** Images showing the good adhesion and conformability of the intrinsically stretchable OFETs on the back of a hand. Reproduced with permission[26]. Copyright 2017, American Association for the Advancement of Science. **c** An integrative platform consisting of an ultra-thin display layer and an ultra-thin electronic sensor layer for smart skin. Reproduced with permission[176]. Copyright 2018, Wiley-VCH. **d** Photograph of a fully printed 10×6 flexible transistor arrays worn on a finger. Reproduced with permission[178]. Copyright 2016, Wiley-VCH. **e** Photograph of an intrinsically stretchable inkjet-printed synaptic transistor array attached on a hand. Reproduced with permission[179]. Copyright 2019, Springer Nature. **f** Self-healing behavior of the damaged PDMS–MPU$_x$–IU$_{1-x}$ polymer film under water environment (top), and high stretching strain of the self-healed polymer film. **g** Optical microscope of a 7 × 7 strain sensor array based on the PDMS–MPU$_x$–IU$_{1-x}$ polymer film for the detection of a metal ball. Reproduced with permission[16]. Copyright 2018, Wiley-VCH. **h** Transfer characteristics curves of an edible OFET on a rigid gelatine capsule substrate. Reproduced with permission[184]. Copyright 2010, Wiley-VCH.

increasing the dynamic non-covalent crosslinking of polymer semiconductor film.

Biocompatibility and biodegradability

Good biocompatibility ensures an intimate association between e-skins and soft body tissues, and good biodegradability ensures a spontaneous degradation of e-skins in or on human body without the additional risk associated with secondary surgeries. For organic materials, the chemical composition, surface charge, and pH value significantly impact their biocompatibility owing to the increased cytotoxicity[182]. PEDOT and its derivatives are desirable biocompatible materials[183]. The substrate, dielectric, and semi-conductor materials from nature showed a great potential for enabling fully biocompatible and biodegradable organic electronics. Irimia-Vladu and coworkers[184] have reported an edible OFET with good biocompatibility, biodegradability, and electrical properties using a wide range of natural materials (Fig. 6h).

Self-powering

The demand for persistent power consumption largely limits the practical application of e-skin. Therefore, preparing a self-powered electronic device is a significant consideration for these e-skins. Some existing electronic devices, such as solar cells, super-capacitors, wireless antennas, piezoelectric nanogenerators and triboelectric generators, have distinct advantages in self-powering application[185,186].

SUMMARY AND PERSPECTIVE

In the past twenty years, a great deal of research efforts on material design, device architecture, and processing technologies have facilitated the rapid development of flexible electronics. The performance of a few reported flexible electronic systems, including displays and biosensors, has reached the same level of the rigid counterparts. Their mechanical compliance and stability can also satisfy the requirements for practical applications. However, there is still a long way to go before the extensive practical applications of FOFETs with regard to the following technical limitations and issues.

Firstly, it remains a considerable challenge to balance the electrical performance and mechanical compliance of organic semiconductors. Geometric engineering is the most commonly used strategy to increase the mechanical flexibility of organic semiconductors, but this strategy usually requires complicated manufacturing processes and is detrimental to the large-area array and integration. Blending with elastomers is considered as an efficient approach to improving the flexibility and stretchability of organic semiconductors with little of sacrifice of the electrical performance. However, current reports only involved the specific elastomers (PDMS, SEBS) and polymer semiconductors (DPP-based

polymers, P3HT), and the blending mechanism is still not clear. Thus, determining the effects of blending conditions (including molecular weight, surface energy, solubility coefficient, phase separation, etc.) on hybrid polymer semiconductor can provide a clear guideline for enabling highly stretchable organic semiconductors. The crosslinking of polymer dielectrics is a feasible method to improve their stretchability and solvent tolerance. In addition, the required intrinsic flexibility and stretchability for all the components largely restrict the application of some rigid functional materials (such as perovskite with excellent light sensitivity) in the stretchable electronic devices due to their high-crystallinity nature. Therefore, how to develop a wide range of multi-functional materials with high flexibility and stretchability is a focus.

Secondly, developing large-scale, low-voltage and solution-processable organic circuits are highly desirable for flexible electronic applications. Most of the reported organic circuits is prepared with organic molecules as the active layer, whereas polymer semiconductors are rarely used in the organic circuits. Moreover, due to the lack of high-performance, air-stable n-type and ambipolar-conjugated polymers, the development of complementary organic circuits lags far behind the unipolar organic circuits. Nowadays, there are two major issues deserving to be addressed: the one is to fabricate high-performance and air-stable n-type and ambipolar polymer semiconductors for solution-processable complementary organic circuits, and the other is to construct highly flexible and stretchable organic circuitry system on ultra-thin plastic or elastomeric substrate.

Thirdly, researchers are encouraged to pioneer the application of FOFETs into complicated integrated systems and subsequent practically applicable e-skins. The commonly used device manufacturing technologies such as spin-coating and vacuum evaporation cannot meet the requirements of large-area and integrated electronic circuitry. Thus, researchers should attach their importance to develop new processing technologies, such as R2R manufacturing. Low-thickness, light weight, high-density and highly flexible electronic devices are also a significant development direction in the future. Moreover, current researches only stayed in the stretchable OFETs, but the preparation of stretchable OFET-based sensors is rarely achieved. Most stretchable OFETs reported are prepared typically based on the continuous thermal lamination-transfer procedures to avoid the solvent damage to adjacent layer. But the complicated manufacturing procedures are also detrimental to the high density and integration. For fabrication of high-performance e-skins, the crosslinking polymer layer is seen as a feasible strategy to overcome this problem.

Fourthly, to surpass the multifunctionalities of human skin and follow the advent of the era of artificial intelligence, e-skins propose higher requirements for flexible electronics and circuits, not just high flexibility and electrical characteristics. Using novel materials and developing efficient device architecture to open up more potential applications in biomedical fields is highly required. For example, how to exploit the existing materials from nature and human body (such as protein, starches and glucose) to prepare highly sensitive and easily degradable biosensors. How to enable the real-time detection of the wound by a highly sensitive, self-healing, and biocompatible OFET-based biosensors. How to integrate various types of FOFET-based biosensors into a device to achieve multivariate change detection. How to achieve a long-lasting sensing and detection for human body by preparing a self-powering FOFET-based sensors. All of these challenges give us more opportunities to explore more innovative applications for flexible electronics. We believe that the application of FOFETs and their circuits in rollable displays, smart cards, and artificial skins will be an increasingly significant interdisciplinary topic in the near future.

REFERENCES
1. Someya, T., Bao, Z. & Malliaras, G. G. The rise of plastic bioelectronics. *Nature* **540**, 379–385 (2016).
2. Bao, Z. & Chen, X. Flexible and stretchable devices. *Adv. Mater.* **28**, 4177–4179 (2016).
3. Han, S.-T. et al. An overview of the development of flexible sensors. *Adv. Mater.* **29**, 1700375 (2017).
4. Ling, H., Liu, S., Zheng, Z. & Yan, F. Organic flexible electronics. *Small Methods* **2**, 1800070 (2018).
5. Guo, X. et al. Current status and opportunities of organic thin-film transistor technologies. *IEEE Trans. Electron Dev.* **64**, 1906–1921 (2017).
6. Yagi, I. et al. A flexible full-color AMOLED display driven by OTFTs. *J. Soc. Inf. Disp.* **16**, 15–20 (2012).
7. Baumbauer, C. L. et al. Printed, flexible, compact UHF-RFID sensor tags enabled by hybrid electronics. *Sci. Rep.* **10**, 16543 (2020).
8. Kwon, J. et al. Three-dimensional monolithic integration in flexible printed organic transistors. *Nat. Commun.* **10**, 54 (2019).
9. Zang, Y. et al. Flexible suspended gate organic thin-film transistors for ultra-sensitive pressure detection. *Nat. Commun.* **6**, 6269 (2015).
10. Wu, W. et al. Ultrathin and conformable lead halide perovskite photodetector arrays for potential application in retina-like vision sensing. *Adv. Mater.* **33**, 2006006 (2021).
11. Muth, J. T. et al. Embedded 3D printing of strain sensors within highly stretchable elastomers. *Adv. Mater.* **26**, 6307–6312 (2014).
12. Kim, J. et al. Wearable smart sensor systems integrated on soft contact lenses for wireless ocular diagnostics. *Nat. Commun.* **8**, 14997 (2017).
13. Xu, W., Min, S.-Y., Hwang, H. & Lee, T.-W. Organic core-sheath nanowire artificial synapses with femtojoule energy consumption. *Sci. Adv.* **2**, e1501326 (2016).
14. Wang, X., Gu, Y., Xiong, Z. & Zhang, T. Silk-molded flexible, ultrasensitive, and highly stable electronic skin for monitoring human physiological signals. *Adv. Mater.* **26**, 1336–1342 (2014).
15. Guan, Y. S. et al. Air/water interfacial assembled rubbery semiconducting nanofilm for fully rubbery integrated electronics. *Sci. Adv.* **6**, eabb3656 (2020).
16. Kang, J. et al. Tough and water-insensitive self-healing elastomer for robust electronic skin. *Adv. Mater.* **30**, 1706846 (2018).
17. Yu, X. et al. Flexible spray-coated TIPS-pentacene organic thin-film transistors as ammonia gas sensors. *J. Mater. Chem. C* **1**, 6532 (2013).
18. Oh, J. Y. et al. Intrinsically stretchable and healable semiconducting polymer for organic transistors. *Nature* **539**, 411–415 (2016).
19. Mun, J. et al. Conjugated carbon cyclic nanorings as additives for intrinsically stretchable semiconducting polymers. *Adv. Mater.* **31**, 1903912 (2019).
20. Chortos, A. et al. Highly stretchable transistors using a microcracked organic semiconductor. *Adv. Mater.* **26**, 4253–4259 (2014).
21. Sun, Y., Choi, W. M., Jiang, H., Huang, Y. Y. & Rogers, J. A. Controlled buckling of semiconductor nanoribbons for stretchable electronics. *Nat. Nanotechnol.* **1**, 201–207 (2006).
22. Huang, Y. et al. Printable low power organic transistor technology for customizable hybrid integration towards internet of everything. *IEEE J. Electron Devices* **8**, 1219–1226 (2020).
23. Huang, Y. et al. Scalable processing of low voltage organic field effect transistors with a facile soft-contact coating approach. *IEEE Electron. Device Lett.* **40**, 1945–1948 (2019).
24. Sandström, A., Dam, H. F., Krebs, F. C. & Edman, L. Ambient fabrication of flexible and large-area organic light-emitting devices using slot-die coating. *Nat. Commun.* **3**, 1002 (2012).
25. Khim, D. et al. Precisely controlled ultrathin conjugated polymer films for large area transparent transistors and highly sensitive chemical sensors. *Adv. Mater.* **28**, 2752–2759 (2016).
26. Xu, J. et al. Highly stretchable polymer semiconductor films through the nanoconfinement effect. *Science* **355**, 59–64 (2017).
27. Xu, J. et al. Multi-scale ordering in highly stretchable polymer semiconducting films. *Nat. Mater.* **18**, 1 (2019).
28. Li, M. et al. Facile four-mask processes for organic thin-film transistor integration structure with metal interconnect. *IEEE Electron. Device Lett.* **41**, 70–72 (2020).

29. Chua, L.-L., Friend, R. H. & Ho, P. K. H. Organic double-gate field-effect transistors: logic-AND operation. *Appl. Phys. Lett.* **87**, 253512 (2005).

30. Hyun, W. J. et al. Printed, self-aligned side-gate organic transistors with a sub-5 m gate-channel distance on imprinted plastic substrates. *Adv. Electron. Mater.* **2**, 1600293 (2016).

31. Koopman, W.-W. A. et al. Contact resistance in ambipolar organic field-effect transistors measured by confocal photoluminescence electro-modulation microscopy. *ACS Appl. Mater. Interfaces* **10**, 35411–35419 (2018).

32. Olivier, Y. et al. 25th Anniversary Article: High-mobility hole and electron transport conjugated polymers: how structure defines function. *Adv. Mater.* **26**, 2119–2136 (2014).

33. Pan, Y. et al. An insight into the role of side chains in the microstructure and carrier mobility of high-performance conjugated polymers. *Poly. Chem.* **12**, 2471–2480 (2021).

34. Wang, C., Dong, H., Hu, W., Liu, Y. & Zhu, D. Semiconducting π-conjugated systems in field-effect transistors: a material odyssey of organic electronics. *Chem. Rev.* **112**, 2208–2267 (2011).

35. Nakayama, K. et al. Patternable solution-crystallized organic transistors with high charge carrier mobility. *Adv. Mater.* **23**, 1626–1629 (2011).

36. Zhao, X., Ding, X., Tang, Q., Tong, Y. & Liu, Y. Photolithography-compatible conformal electrodes for high-performance bottom-contact organic single-crystal transistors. *J. Mater. Chem. C* **5**, 12699–12706 (2017).

37. Minemawari, H. et al. Inkjet printing of single-crystal films. *Nature* **475**, 364–367 (2011).

38. Reyes-Martinez, M. A., Crosby, A. J. & Briseno, A. L. Rubrene crystal field-effect mobility modulation via conducting channel wrinkling. *Nat. Commun.* **6**, 6948 (2015).

39. Wang, Y. et al. Organic crystalline materials in flexible electronics. *Chem. Soc. Rev.* **48**, 1492–1530 (2019).

40. Onorato, J., Pakhnyuk, V. & Luscombe, C. K. Structure and design of polymers for durable, stretchable organic electronics. *Poly. J.* **49**, 41–60 (2017).

41. O'Connor, B. et al. Correlations between mechanical and electrical properties of polythiophenes. *ACS Nano* **4**, 7538–7544 (2010).

42. Wu, H.-C. et al. A rapid and facile soft contact lamination method: evaluation of polymer semiconductors for stretchable transistors. *Chem. Mater.* **26**, 4544–4551 (2014).

43. Müller, C. et al. Tough, semiconducting polyethylene-poly(3-hexylthiophene) diblock copolymers. *Adv. Funct. Mater.* **17**, 2674–2679 (2007).

44. Peng, R. et al. An ABA triblock copolymer strategy for intrinsically stretchable semiconductors. *J. Mater. Chem. C* **3**, 3599–3606 (2015).

45. Son, S. Y. et al. High-field-effect mobility of low-crystallinity conjugated polymers with localized aggregates. *J. Am. Chem. Soc.* **138**, 8096–8103 (2016).

46. Kang, I., Yun, H.-J., Chung, D. S., Kwon, S.-K. & Kim, Y.-H. Record high hole mobility in polymer semiconductors via side-chain engineering. *J. Am. Chem. Soc.* **135**, 14896–14899 (2013).

47. Wen, H.-F. et al. Soft poly(butyl acrylate) side chains toward intrinsically stretchable polymeric semiconductors for field-effect transistor applications. *Macromolecules* **50**, 4982–4992 (2017).

48. Koch, F. P. V. et al. The impact of molecular weight on microstructure and charge transport in semicrystalline polymer semiconductors–poly(3-hexylthiophene), a model study. *Prog. Polym. Sci.* **38**, 1978–1989 (2013).

49. Kim, J.-S. et al. Tuning mechanical and optoelectrical properties of poly(3-hexylthiophene) through systematic regioregularity control. *Macromolecules* **48**, 4339–4346 (2015).

50. Mun, J. et al. F4-TCNQ as an additive to impart stretchable semiconductors with high mobility and stability. *Adv. Electron. Mater.* **6**, 2000251 (2020).

51. Shin, M. et al. Polythiophene nanofibril bundles surface-embedded in elastomer: a route to a highly stretchable active channel layer. *Adv. Mater.* **27**, 1255–1261 (2015).

52. Nikzad, S. et al. Inducing molecular aggregation of polymer semiconductors in a secondary insulating polymer matrix to enhance charge transport. *Chem. Mater.* **32**, 897–905 (2020).

53. Yang, C. et al. Hybrid films: Kirigami-inspired deformable 3D structures conformable to curved biological surface. *Adv. Sci.* **5**, 1870073 (2018).

54. Chen, D., Liang, J. & Pei, Q. Flexible and stretchable electrodes for next generation polymer electronics: a review. *Sci. China Chem.* **59**, 659–671 (2016).

55. Huang, S., Liu, Y., Zhao, Y., Ren, Z. & Guo, C. F. Flexible electronics: stretchable electrodes and their future. *Adv. Funct. Mater.* **29**, 1805924 (2019).

56. Liu, K., Guo, Y. L. & Liu, Y. Q. Recent progress in stretchable organic field-effect transistors. *Sci. China Technol. Sci.* **62**, 1255–1276 (2019).

57. Xiang, L., Zhang, H., Hu, Y. & Peng, L.-M. Carbon nanotube-based flexible electronics. *J. Mater. Chem. C* **6**, 7714–7727 (2018).

58. Guo, C. F. & Ren, Z. Flexible transparent conductors based on metal nanowire networks. *Mater. Today* **18**, 143–154 (2015).

59. Hu, L., Han, S. K., Lee, J. Y., Peumans, P. & Cui, Y. Scalable coating and properties of transparent, flexible, silver nanowire electrodes. *ACS Nano* **4**, 2955–2963 (2010).

60. Kang, M. et al. Synergistic high charge-storage capacity for multi-level flexible organic flash memory. *Sci. Rep.* **5**, 12299 (2015).

61. Kim, J.-Y. & Jang, K.-S. Facile fabrication of stretchable electrodes by sedimentation of Ag nanoparticles in PDMS matrix. *J. Nanomater.* **2018**, 1–6 (2018).

62. Park, J. H. et al. Flash-induced self-limited plasmonic welding of silver nanowire network for transparent flexible energy harvester. *Adv. Mater.* **29**, 1603473 (2016).

63. Lee, P. et al. Highly stretchable and highly conductive metal electrode by very long metal nanowire percolation network. *Adv. Mater.* **24**, 3326–3332 (2012).

64. Wang, H., Lin, J. & Shen, Z. X. Polyaniline (PANi) based electrode materials for energy storage and conversion. *J. Sci. Adv. Mater. Dev.* **1**, 225–255 (2016).

65. Kang, H., Jung, S., Jeong, S., Kim, G. & Lee, K. Polymer-metal hybrid transparent electrodes for flexible electronics. *Nat. Commun.* **6**, 6503 (2015).

66. Vosgueritchian, M., Lipomi, D. J. & Bao, Z. Highly conductive and transparent PEDOT:PSS films with a fluorosurfactant for stretchable and flexible transparent electrodes. *Adv. Funct. Mater.* **22**, 421–428 (2011).

67. Lang, U., Naujoks, N. & Dual, J. Mechanical characterization of PEDOT:PSS thin films. *Synth. Met.* **159**, 473–479 (2009).

68. Niu, T. Carbon nanotubes advance next-generation electronics. *Nano Today* **35**, 100992 (2020).

69. Lipomi, D. J. et al. Skin-like pressure and strain sensors based on transparent elastic films of carbon nanotubes. *Nat. Nanotechnol.* **6**, 788–792 (2011).

70. Shin, M. K. et al. Elastomeric conductive composites based on carbon nanotube forests. *Adv. Mater.* **22**, 2663–2667 (2010).

71. Bae, S. et al. Roll-to-roll production of 30-inch graphene films for transparent electrodes. *Nat. Nanotechnol.* **5**, 574–578 (2010).

72. Nicholl, R. J. T. et al. The effect of intrinsic crumpling on the mechanics of free-standing graphene. *Nat. Commun.* **6**, 8789 (2015).

73. Hong, J.-Y., Kim, W., Choi, D., Kong, J. & Park, H. S. Omnidirectionally stretchable and transparent graphene electrodes. *ACS Nano* **10**, 9446–9455 (2016).

74. Park, J.-Y. & Kim, H.-K. Highly stretchable polymer-dispersed liquid crystal-based smart windows with transparent and stretchable hybrid electrodes. *RSC Adv.* **8**, 36549–36557 (2018).

75. Lee, P. et al. Highly stretchable or transparent conductor fabrication by a hierarchical multiscale hybrid nanocomposite. *Adv. Funct. Mater.* **24**, 5671–5678 (2014).

76. Choi, T. Y. et al. Stretchable, transparent, and stretch-unresponsive capacitive touch sensor array with selectively patterned silver nanowires/reduced graphene oxide electrodes. *ACS Appl. Mater. Inter.* **9**, 18022–18030 (2017).

77. Keplinger, C. et al. Stretchable, transparent, ionic conductors. *Science* **341**, 984–987 (2013).

78. Dickey, M. D. Stretchable and soft electronics using liquid metals. *Adv. Mater.* **29**, 1606425 (2017).

79. Wang, B. et al. High-k gate dielectrics for emerging flexible and stretchable electronics. *Chem. Rev.* **118**, 5690–5754 (2018).

80. Rao, Y.-L. et al. Stretchable self-healing polymeric dielectrics cross-linked through metal–ligand coordination. *J. Am. Chem. Soc.* **138**, 6020–6027 (2016).

81. Wang, S. et al. Skin electronics from scalable fabrication of an intrinsically stretchable transistor array. *Nature* **555**, 83–88 (2018).

82. Drury, C. J., Mutsaers, C. M. J., Hart, C. M., Matters, M. & de Leeuw, D. M. Low-cost all-polymer integrated circuits. *Appl. Phys. Lett.* **73**, 108–110 (1998).

83. Huang, Z. et al. Three-dimensional integrated stretchable electronics. *Nat. Electron.* **1**, 473–480 (2018).

84. Bode, D. et al. Noise-margin analysis for organic thin-film complementary technology. *IEEE Trans. Electron. Devices* **57**, 201–208 (2010).

85. Fukuda, K. et al. Organic pseudo-CMOS circuits for low-voltage large-gain high-speed operation. *IEEE Electron. Device Lett.* **32**, 1448–1450 (2011).

86. Han, L. et al. Through-plastic-via three-dimensional integration for integrated organic field-effect transistor bio-chemical sensor chip. *IEEE Electron. Device Lett.* **42**, 569–572 (2021).

87. Fiore, V. et al. An integrated 13.56-MHz RFID tag in a printed organic complementary TFT technology on flexible substrate. *IEEE Trans. Circuits-I* **62**, 1668–1677 (2015).

88. Sugiyama, M. et al. An ultraflexible organic differential amplifier for recording electrocardiograms. *Nat. Electron.* **2**, 351–360 (2019).

89. Shiwaku, R. et al. A printed organic amplification system for wearable potentiometric electrochemical sensors. *Sci. Rep.* **8**, 3922 (2018).

90. Yagi, I. et al. Distinguished Paper: a full-color, top-emission AM-OLED display driven by OTFTs. *SID Symp. Dig. Tech. Pap.* **38**, 1753–1756 (2007).

91. Yoshida, A. et al. 3-inch full-color OLED display using a plastic substrate. *SID '03 Dig.* **34**, 856–859 (2003).

92. Gelinck, G. H. et al. Flexible active-matrix displays and shift registers based on solution-processed organic transistors. *Nat. Mater.* **3**, 106–110 (2004).

93. Choi, M.-C., Kim, Y. & Ha, C.-S. Polymers for flexible displays: from material selection to device applications. *Prog. Polym. Sci.* **33**, 581–630 (2008).

94. Huitema, H. E. A. et al. Plastic transistors in active-matrix displays. *Nature* **414**, 599 (2001).

95. Noda, M. et al. 47.3: A rollable AM-OLED display driven by OTFTs. *SID Symp. Dig. Tech. Pap.* **41**, 710 (2010).

96. Yin, D. et al. Efficient and mechanically robust stretchable organic light-emitting devices by a laser-programmable buckling process. *Nat. Commun.* **7**, 11573 (2016).

97. Liang, J. et al. Silver nanowire percolation network soldered with graphene oxide at room temperature and its application for fully stretchable polymer light-emitting diodes. *ACS Nano* **8**, 1590–1600 (2014).

98. Kim, T., Lee, H., Jo, W., Kim, T.-S. & Yoo, S. Realizing stretchable OLEDs: a hybrid platform based on rigid island arrays on a stress-relieving bilayer structure. *Adv. Mater. Technol.* **5**, 2000494 (2020).

99. Mishima, T., Abe, N., Tanaka, K. & Taki, H. Toward construction of a mobile system with long-range RFID sensors. *IEEE Conf. Cybern. Intell. Syst.* **2**, 960–965 (2004).

100. Sarangan, V., Devarapalli, M. R. & Radhakrishnan, S. A framework for fast RFID tag reading in static and mobile environments. *Comput. Netw.* **52**, 1058–1073 (2008).

101. Simplot-Ryl, D., Stojmenovic, I., Micic, A. & Nayak, A. A hybrid randomized protocol for RFID tag identification. *Sens. Rev.* **26**, 147–154 (2006).

102. Jung, M. et al. All-printed and roll-to-roll-printable 13.56-MHz-operated 1-bit RF tag on plastic foils. *IEEE Trans. Electron Device* **57**, 571–580 (2010).

103. Yang, L., Rida, A., Vyas, R. & Tentzeris, M. M. RFID tag and RF structures on a paper substrate using inkjet-printing technology. *IEEE Trans. Microw. Theory* **55**, 2894–2901 (2007).

104. Trung, T. Q., Ramasundaram, S., Hwang, B.-U. & Lee, N.-E. An all-elastomeric transparent and stretchable temperature sensor for body-attachable wearable electronics. *Adv. Mater.* **28**, 502–509 (2015).

105. Rim, Y. S., Bae, S.-H., Chen, H., De Marco, N. & Yang, Y. Recent progress in materials and devices toward printable and flexible sensors. *Adv. Mater.* **28**, 4415–4440 (2016).

106. Someya, T., Dodabalapur, A., Huang, J., See, K. C. & Katz, H. E. Chemical and physical sensing by organic field-effect transistors and related devices. *Adv. Mater.* **22**, 3799–3811 (2010).

107. Zang, Y., Huang, D., Di, C. & Zhu, D. Device engineered organic transistors for flexible sensing applications. *Adv. Mater.* **28**, 4549–4555 (2016).

108. Huang, W. et al. Highly sensitive NH3 detection based on organic field-effect transistors with tris(pentafluorophenyl)borane as receptor. *J. Am. Chem. Soc.* **134**, 14650–14653 (2012).

109. Huang, J. et al. Direct detection of dilute solid chemicals with responsive lateral organic diodes. *J. Am. Chem. Soc.* **139**, 12366–12369 (2017).

110. Li, L. et al. High-performance field-effect ammonia sensors based on a structured ultrathin organic semiconductor film. *Adv. Mater.* **25**, 3419–3425 (2013).

111. Shi, W., Guo, Y. & Liu, Y. When flexible organic field-effect transistors meet biomimetics: a prospective view of the internet of things. *Adv. Mater.* **32**, 1901493 (2019).

112. Yan, F. et al. Polycrystalline silicon ion sensitive field effect transistors. *Appl. Phys. Lett.* **86**, 053901 (2005).

113. Furusawa, H. et al. Detection of 1,5-anhydroglucitol as a biomarker for diabetes using an organic field-effect transistor-based biosensor. *Technologies* **6**, 77 (2018).

114. Elkington, D., Belcher, W. J., Dastoor, P. C. & Zhou, X. J. Detection of saliva-range glucose concentrations using organic thin-film transistors. *Appl. Phys. Lett.* **105**, 043303 (2014).

115. Roberts, M. E. et al. Water-stable organic transistors and their application in chemical and biological sensors. *Proc. Natl Acad. Sci. USA* **105**, 12134–12139 (2008).

116. Roberts, M. E., Mannsfeld, S. C. B., Stoltenberg, R. M. & Bao, Z. Flexible, plastic transistor-based chemical sensors. *Org. Electron.* **10**, 377–383 (2009).

117. Ji, T., Rai, P., Jung, S. & Varadan, V. K. In vitro evaluation of flexible pH and potassium ion-sensitive organic field effect transistor sensors. *Appl. Phys. Lett.* **92**, 233304 (2008).

118. Feili, D., Schuettler, M., Doerge, T., Kammer, S. & Stieglitz, T. Encapsulation of organic field effect transistors for flexible biomedical microimplants. *Sensors Actuat. A Phys.* **120**, 101–109 (2005).

119. Huang, X., Ji, D., Fuchs, H., Hu, W. & Li, T. Recent progress in organic photo-transistors: semiconductor materials, device structures and optoelectronic applications. *ChemPhotoChem* **4**, 3 (2019).

120. Rim, Y. S. et al. Ultrahigh and broad spectral photodetectivity of an organic-inorganic hybrid phototransistor for flexible electronics. *Adv. Mater.* **27**, 6885–6891 (2015).

121. Baeg, K.-J., Binda, M., Natali, D., Caironi, M. & Noh, Y.-Y. Organic light detectors: photodiodes and phototransistors. *Adv. Mater.* **25**, 4267–4295 (2013).

122. Rogers, J. A., Someya, T. & Huang, Y. Materials and mechanics for stretchable electronics. *Science* **327**, 1603–1607 (2010).

123. Chen, Y., Chu, Y., Wu, X., Ou-Yang, W. & Huang, J. High-performance inorganic perovskite quantum dot-organic semiconductor hybrid phototransistors. *Adv. Mater.* **29**, 1704062 (2017).

124. Zou, C. et al. A highly sensitive UV-vis-NIR all-inorganic perovskite quantum dot phototransistor based on a layered heterojunction. *Adv. Opt. Mater.* **6**, 1800324 (2018).

125. Liguori, R., Sheets, W. C., Facchetti, A. & Rubino, A. Light- and bias-induced effects in pentacene-based thin film phototransistors with a photocurable polymer dielectric. *Org. Electron.* **28**, 147–154 (2016).

126. Gu, P., Yao, Y., Feng, L., Niu, S. & Dong, H. Recent advances in polymer photo-transistors. *Polym. Chem.* **6**, 7933–7944 (2015).

127. Shockley, W., Sparks, M. & Teal, G. K. p–n junction transistors. *Phys. Rev.* **83**, 151–162 (1951).

128. Li, M. et al. Phenanthrene condensed thiadiazoloquinoxaline donor–acceptor polymer for phototransistor applications. *Chem. Mater.* **27**, 2218–2223 (2015).

129. Liu, Y. et al. High performance photoswitches based on flexible and amorphous D-A polymer nanowires. *Small* **9**, 294–299 (2012).

130. Zhu, M. et al. Enhanced near-infrared photoresponse of organic phototransistors based on single-component donor–acceptor conjugated polymer nanowires. *Nanoscale* **8**, 7738–7748 (2016).

131. Li, Q. et al. Recent advances in one-dimensional organic p–n heterojunctions for optoelectronic device applications. *J. Mater. Chem. C* **4**, 9388–9398 (2016).

132. Xie, C. & Yan, F. Perovskite/poly(3-hexylthiophene)/graphene multi-heterojunction phototransistors with ultrahigh gain in broadband wavelength region. *ACS Appl. Mater. Interfaces* **9**, 1569–1576 (2017).

133. Yu, Y. et al. Broadband phototransistor based on CH3NH3PbI3 perovskite and PbSe quantum dot heterojunction. *J. Phys. Chem. Lett.* **8**, 445–451 (2017).

134. Trung, T. Q. et al. An omnidirectionally stretchable photodetector based on organic–inorganic heterojunctions. *ACS Appl. Mater. Interfaces* **9**, 35958–35967 (2017).

135. Liu, K. et al. Carbon nanotube-based van der Waals heterojunction electrodes for high-performance intrinsically stretchable organic photoelectric transistors. *Giant* **7**, 100060 (2021).

136. Chow, P. C. Y. et al. Dual-gate organic phototransistor with high-gain and linear photoresponse. *Nat. Commun.* **9**, 4546 (2018).

137. Wang, H. et al. Inkjet printing short-channel polymer transistors with high-performance and ultrahigh photoresponsivity. *Adv. Mater.* **26**, 4683–4689 (2014).

138. Zhang, G. et al. High-performance organic phototransistors with vertical structure design. *IEEE Trans. Electron Device* **6**, 1–4 (2019).

139. Demchyshyn, S. et al. Designing ultraflexible perovskite X-ray detectors through interface engineering. *Adv. Sci.* **7**, 2002586 (2020).

140. Chu, Y. et al. Photosensitive and flexible organic field-effect transistors based on interface trapping effect and their application in 2D imaging array. *Adv. Sci.* **3**, 1500435 (2016).

141. Lee, M. Y. et al. Highly flexible organic nanofiber phototransistors fabricated on a textile composite for wearable photosensors. *Adv. Funct. Mater.* **26**, 1445–1453 (2016).

142. Baeg, K.-J., Noh, Y.-Y., Ghim, J., Lim, B. & Kim, D.-Y. Polarity effects of polymer gate electrets on non-volatile organic field-effect transistor memory. *Adv. Funct. Mater.* **18**, 3678–3685 (2008).

143. Chou, Y.-H., Chang, H.-C., Liu, C.-L. & Chen, W.-C. Polymeric charge storage electrets for non-volatile organic field effect transistor memory devices. *Polym. Chem.* **6**, 341–352 (2015).

144. Ni, Y., Wang, Y. & Xu, W. Recent process of flexible transistor-structured memory. *Small* **4**, 1905332 (2020).

145. Han, S. T., Ye, Z. & Roy, V. Towards the development of flexible non-volatile memories. *Adv. Mater.* **25**, 5425–5449 (2013).

146. Lee, S., Seong, H., Im, S. G., Moon, H. & Yoo, S. Organic flash memory on various flexible substrates for foldable and disposable electronics. *Nat. Commun.* **8**, 725 (2017).

147. Kang, M., Baeg, K.-J., Khim, D., Noh, Y.-Y. & Kim, D.-Y. Printed, flexible, organic nano-floating-gate memory: effects of metal nanoparticles and blocking dielectrics on memory characteristics. *Adv. Funct. Mater.* **23**, 3503–3512 (2013).

148. Leong, W. L. et al. Non-volatile organic memory applications enabled by in situ synthesis of gold nanoparticles in a self-assembled block copolymer. *Adv. Mater.* **20**, 2325–2331 (2008).

149. Zhang, L. et al. Large-area, flexible imaging arrays constructed by light-charge organic memories. *Sci. Rep.* **3**, 1080 (2013).

150. Wu, C., Wang, W. & Song, J. Solution processed top-gate high-performance organic transistor nonvolatile memory with separated molecular microdomains floating-gate. *IEEE Electron. Device Lett.* **38**, 641–644 (2017).

151. Li, J. & Yan, F. Solution-processable low-voltage and flexible floating-gate memories based on an n-type polymer semiconductor and high-κ polymer gate dielectrics. *ACS Appl. Mater. Interfaces* **6**, 12815–12820 (2014).

152. Han, S.-T. et al. Layer-by-layer-assembled reduced graphene oxide/gold nanoparticle hybrid double-floating-gate structure for low-voltage flexible flash memory. *Adv. Mater.* **25**, 872–877 (2012).

153. Park, Y.-S. & Lee, J.-S. Design of an efficient charge-trapping layer with a built-in tunnel barrier for reliable organic-transistor memory. *Adv. Mater.* **27**, 706–711 (2014).

154. Ling, Q.-D. et al. Polymer electronic memories: materials, devices and mechanisms. *Prog. Polym. Sci.* **33**, 917–978 (2008).

155. Guo, Y. et al. High-performance phototransistors based on organic microribbons prepared by a solution self-assembly process. *Adv. Funct. Mater.* **20**, 1019–1024 (2010).

156. Ling, H. et al. Synergistic effects of self-doped nanostructures as charge trapping elements in organic field effect transistor memory. *ACS Appl. Mater. Interfaces* **8**, 18969–18977 (2016).

157. Yu, A.-D. et al. Multilevel nonvolatile flexible organic field-effect transistor memories employing polyimide electrets with different charge-transfer effects. *Macromol. Rapid Commun.* **35**, 1039–1045 (2014).

158. Hwang, S. K., Bae, I., Kim, R. H. & Park, C. Flexible non-volatile ferroelectric polymer memory with gate-controlled multilevel operation. *Adv. Mater.* **24**, 5910–5914 (2012).

159. Tsai, M.-F. et al. Oxide heteroepitaxy based flexible ferroelectric transistor. *ACS Appl. Mater. Interfaces* **11**, 25882–25890 (2019).

160. Xu, T., Xiang, L., Xu, M., Xie, W. & Wang, W. Excellent low-voltage operating flexible ferroelectric organic transistor nonvolatile memory with a sandwiching ultrathin ferroelectric film. *Sci. Rep.* **7**, 8890 (2017).

161. Izyumskaya, N. et al. Processing, structure, properties, and applications of PZT thin films. *Crit. Rev. Solid State* **32**, 111–202 (2007).

162. Seager, C. H., McIntyre, D. C., Warren, W. L. & Tuttle, B. A. Charge trapping and device behavior in ferroelectric memories. *Appl. Phys. Lett.* **68**, 2660–2662 (1996).

163. Naber, R. C. G. et al. High-performance solution-processed polymer ferroelectric field-effect transistors. *Nat. Mater.* **4**, 243–248 (2005).

164. Asadi, K., de Leeuw, D. M., de Boer, B. & Blom, P. W. M. Organic non-volatile memories from ferroelectric phase-separated blends. *Nat. Mater.* **7**, 547–550 (2008).

165. Baeg, K.-J. et al. Remarkable enhancement of hole transport in top-gated n-type polymer field-effect transistors by a high-k dielectric for ambipolar electronic circuits. *Adv. Mater.* **24**, 5433–5439 (2012).

166. Kodama, H., Takahashi, Y. & Furukawa, T. Effects of annealing on the structure and switching characteristics of VDF/TrFE copolymers. *Ferroelectrics* **203**, 433–455 (1997).

167. Khan, M. A. et al. High-performance ferroelectric memory based on phase-separated films of polymer blends. *Adv. Funct. Mater.* **24**, 1372–1381 (2013).

168. Zhou, Y., Han, S.-T., Xu, Z.-X. & Roy, V. A. L. The strain and thermal induced tunable charging phenomenon in low power flexible memory arrays with a gold nanoparticle monolayer. *Nanoscale* **5**, 1972–1979 (2013).

169. Hu, D., Wang, X., Chen, H. & Guo, T. High performance flexible nonvolatile memory based on vertical organic thin film transistor. *Adv. Funct. Mater.* **27**, 1703541 (2017).

170. Wang, X. et al. Recent progress in electronic skin. *Adv. Sci.* **2**, 1500169 (2015).

171. Lumpkin, E. A. & Caterina, M. J. Mechanisms of sensory transduction in the skin. *Nature* **445**, 858–865 (2007).

172. Pang, C. et al. A flexible and highly sensitive strain-gauge sensor using reversible interlocking of nanofibres. *Nat. Mater.* **11**, 795–801 (2012).

173. Hammock, M. L. et al. 25th Anniversary Article: The evolution of electronic skin (E-skin): a brief history, design considerations, and recent progress. *Adv. Mater.* **25**, 5997–6038 (2013).

174. Chortos, A., Liu, J. & Bao, Z. Pursuing prosthetic electronic skin. *Nat. Mater.* **15**, 937–950 (2016).

175. Lee, J. et al. Conductive fiber-based ultrasensitive textile pressure sensor for wearable electronics. *Adv. Mater.* **27**, 2433–2439 (2015).

176. Koo, J. H., Kim, D. C., Shim, H. J., Kim, T. H. & Kim, D.-H. Flexible and stretchable smart display: materials, fabrication, device design, and system integration. *Adv. Funct. Mater.* **28**, 1801834 (2018).

177. Kim, J. et al. Stretchable silicon nanoribbon electronics for skin prosthesis. *Nat. Commun.* **5**, 5747 (2014).

178. Liang, J., Tong, K. & Pei, Q. A water-based silver-nanowire screen-print ink for the fabrication of stretchable conductors and wearable thin-film transistors. *Adv. Mater.* **28**, 5986–5996 (2016).

179. Molina-Lopez, F. et al. Inkjet-printed stretchable and low voltage synaptic transistor array. *Nat. Commun.* **10**, 2676 (2019).

180. Benight, S. J., Wang, C., Tok, J. B. H. & Bao, Z. Stretchable and self-healing polymers and devices for electronic skin. *Prog. Polym. Sci.* **38**, 1961–1977 (2013).

181. Li, C.-H. et al. A highly stretchable autonomous self-healing elastomer. *Nat. Chem.* **8**, 618–624 (2016).

182. Li, Q. et al. Integrated low voltage ion sensing organic field effect transistor system on plastic. *IEEE Electron. Device Lett.* **39**, 591–594 (2018).

183. Lin, P., Yan, F., Yu, J., Chan, H. L. W. & Yang, M. The application of organic electrochemical transistors in cell-based biosensors. *Adv. Mater.* **22**, 3655–3660 (2010).

184. Irimia-Vladu, M. et al. Biocompatible and biodegradable materials for organic field-effect transistors. *Adv. Funct. Mater.* **20**, 4069–4076 (2010).

185. Wang, Z. L., Chen, J. & Lin, L. Progress in triboelectric nanogenerators as a new energy technology and self-powered sensors. *Energy Environ. Sci.* **8**, 2250–2282 (2015).

186. Pan, C. et al. Generating electricity from biofluid with a nanowire-based biofuel cell for self-powered nanodevices. *Adv. Mater.* **22**, 5388–5392 (2010).

ACKNOWLEDGEMENTS

AUTHOR CONTRIBUTIONS
Y.G. and X.G. proposed and supervised the project. K.L. and B.O. wrote the manuscript. Y.G., X.G., Y.L., and K.L. revised the manuscript.

COMPETING INTERESTS
The authors declare no competing interests.

ADDITIONAL INFORMATION
Correspondence and requests for materials should be addressed to Xiaojun Guo or Yunlong Guo.

Reprints and permission information is available at http://www.nature.com/reprints

Publisher's note Springer Nature remains neutral with regard to jurisdictional claims in published maps and institutional affiliations.